



Observation of electroweak production of $W\gamma$ with two jets in proton-proton collisions at $\sqrt{s} = 13$ TeV

The CMS Collaboration*

Abstract

A first observation is presented for the electroweak production of a W boson, a photon, and two jets in proton-proton collisions. The W boson decays are selected by requiring one identified electron or muon and an imbalance in transverse momentum. The two jets are required to have a high dijet mass and a large separation in pseudorapidity. The measurement is based on data collected with the CMS detector at a center-of-mass energy of 13 TeV, corresponding to an integrated luminosity of 35.9 fb^{-1} . The observed (expected) significance for this process is 4.9 (4.6) standard deviations. After combining with previously reported CMS results at 8 TeV, the observed (expected) significance is 5.3 (4.8) standard deviations. The cross section for the electroweak $W\gamma jj$ production in a restricted fiducial region is measured as $20.4 \pm 4.5 \text{ fb}$ and the total cross section for $W\gamma$ production in association with 2 jets in the same fiducial region is $108 \pm 16 \text{ fb}$. All results are in good agreement with recent theoretical predictions. Constraints are placed on anomalous quartic gauge couplings in terms of dimension-8 effective field theory operators.

Submitted to Physics Letters B

1 Introduction

After the discovery of the Higgs boson at the CERN LHC [1–3], one of the primary goals of high-energy physics is to examine the details of the mechanism of electroweak (EW) symmetry breaking, e.g., through measurements of the properties of the Higgs boson. Vector boson scattering (VBS) processes comprise an independent and complementary method to study EW symmetry breaking. The nonabelian nature of gauge interactions in the standard model (SM) leads to a rich variety of VBS processes with unique features and opportunities to probe physics beyond the SM (BSM).

The high energy and luminosity of the LHC make it possible to study the rare VBS processes in detail. The CMS Collaboration reported the EW production of two W bosons of same electric charge produced in association with two jets ($W^\pm W^\pm jj$), with a significance of 5.5 standard deviations (SD) based on the initial proton-proton (pp) data collected at 13 TeV [4]. There have been additional VBS results from both the ATLAS and CMS Collaborations. Notably, ATLAS observed EW ($W^\pm W^\pm jj$) production with a significance of 6.5 SD [5]. CMS recently reported an observation of WZ VBS events at a significance of 6.8 SD [6], along with further studies in the same ($W^\pm W^\pm jj$) channel, based on data collected at 13 TeV. Moreover, VBS processes involving a photon in the final state, $W\gamma$ and $Z\gamma$ scattering, were also reported by ATLAS and CMS, based on data collected at $\sqrt{s} = 8$ TeV, corresponding to an integrated luminosity of approximately 20 fb^{-1} [7–9]. The observed (expected) significance for $W\gamma$ scattering from CMS was 2.7 (1.5) SD. For $Z\gamma$ scattering ATLAS and CMS observed (expected) significances of 2.0 (1.8) and 3.0 (2.1) SD, respectively, based on the SM prediction. A recent update on $Z\gamma$ scattering from CMS, based on the initial data collected at 13 TeV combined with 8 TeV results [10], reported an observed (expected) significance of 4.7 (5.5) SD.

This paper presents a measurement of VBS in the $W\gamma$ channel at $\sqrt{s} = 13$ TeV. As shown in Fig. 1, the signal process includes both VBS and non-VBS EW diagrams, such as EW contributions through triple and quartic gauge couplings. QCD-induced production of $W\gamma jj$ can also take place, as shown in the diagram on the right, with both jets originating from QCD vertices. The diagrams shown are representative of the many possibilities in the SM. The effects of BSM physics, such as anomalous triple and quartic gauge couplings (aTGC and aQGC), are also possible [11]. While aTGC is well constrained by other processes including Higgs boson and diboson productions, aQGC is more suitable for VBS study.

The data correspond to an integrated luminosity of $35.9 \pm 0.9 \text{ fb}^{-1}$ collected during 2016 using the CMS detector [12] at the LHC. For measuring the EW $W\gamma jj$ production, candidate events are selected by requiring one identified lepton (either an electron or muon), one identified photon, two jets with a large rapidity separation and a large dijet invariant mass (m_{jj}), and a moderate imbalance in transverse momentum, p_T^{miss} . This selection reduces the contribution from the strong (QCD) production of jets produced together with the W boson and the photon, making the experimental signature an ideal topology for VBS $W\gamma$ studies. The interference among the VBS diagrams ensures the unitarity of the VBS cross section in the SM at high energy, and an interference is also expected between QCD and EW processes [13, 14].

2 The CMS detector

The central feature of the CMS [12] apparatus is a superconducting solenoid of 6 m internal diameter, providing a magnetic field of 3.8 T. A silicon pixel and strip tracker, a lead tungstate crystal electromagnetic calorimeter (ECAL), and a brass and scintillator hadron calorimeter (HCAL), each composed of a barrel and two endcap sections reside within the volume of the

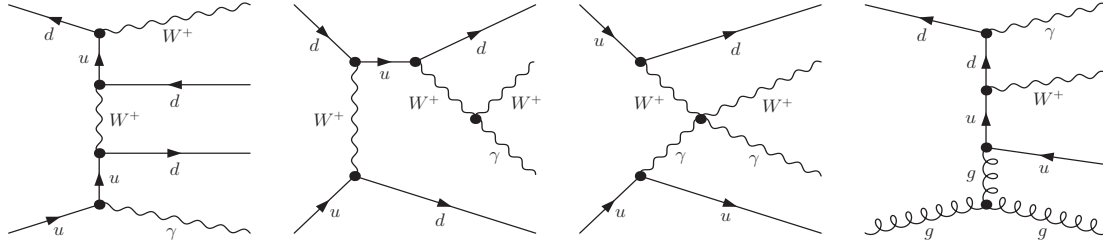


Figure 1: Representative diagrams for $\ell\nu\gamma jj$ production at the LHC for EW production (left), EW production through triple (middle left) and quartic (middle right) gauge boson couplings, and QCD-induced processes (right).

solenoid. Forward calorimeters extend the coverage provided by the barrel and endcap detectors up to a pseudorapidity of $|\eta| = 5$. Muons are detected in gas-ionization chambers embedded in the steel flux-return yoke outside the solenoid.

Events of interest are selected using a two-tiered trigger system [15]. The first level (L1), composed of specialized hardware processors, uses information from the calorimeters and muon detectors to select events at a rate of around 100 kHz with a latency of $4 \mu\text{s}$. The second level consists of a farm of processors running a version of the full event reconstruction software optimized for fast processing that reduces the event rate to around 1 kHz before data storage.

A more detailed description of the CMS detector, together with a definition of the coordinate system and kinematic variables, can be found in Ref. [12].

3 Signal and background simulation

The signal and background processes are simulated using the Monte Carlo (MC) generator MADGRAPH5_aMC@NLO (MG5) [16]. The EW $W\gamma jj$ signal is simulated at leading order (LO) using version 2.6.0. The main background from QCD $W\gamma$ is simulated with up to one jet in the matrix element calculation at next-to-leading order (NLO) with version 2.4.2, using the FxFx scheme [17] to merge jets from the matrix element calculation and parton showering. The interference between the EW and QCD processes is predicted to 1–3% in the signal region and is treated as a systematic uncertainty. Other background contributions include diboson VV processes (WW , WZ , ZZ) simulated at LO with PYTHIA 8.212 [18], single top quark processes simulated with POWHEG 2.0 [19], and $t\bar{t}\gamma$ production simulated at NLO with MG5 using the FxFx jet merging scheme. Cross sections evaluated at NLO in the QCD coupling strength (α_S) are used to normalize these simulated event samples.

The PYTHIA package, with the CUETP8M1 [20, 21] tune, is used for parton showering, hadronization, and underlying-event simulation. The NNPDF 3.0 set [22] of parton distribution functions (PDFs) is used as default. All simulated events are processed through a GEANT4 [23] simulation of the CMS detector. Factors determined by a tag-and-probe technique [24] are used to correct the differences between data and simulation in the trigger efficiency, as well as the reconstruction and identification (ID) efficiencies. Additional overlapping pp interactions (pileup) are superimposed over the hard scattering interaction with a distribution of primary vertices matching that obtained from the collision data. The MC samples are analyzed using the same procedures as the data.

4 Event reconstruction

The particle-flow (PF) algorithm [25] reconstructs and identifies each individual particle in an event, through an optimized combination of information from the various elements of the CMS detector. The energy of photons is obtained from the ECAL measurement. The energy of electrons is determined from a combination of the electron momentum at the primary interaction vertex as determined in the tracker, the energy of the corresponding ECAL cluster, and the energy sum of all bremsstrahlung photons spatially compatible with originating from the electron track. The energy of muons is obtained from the curvature of the corresponding track. The energy of charged hadrons is determined from a combination of their momentum measured in the tracker and the matching ECAL and HCAL energy depositions, corrected for the response of the calorimeters to hadronic showers. Finally, the energy of neutral hadrons is obtained from the corresponding corrected ECAL and HCAL energies. The PF candidates are used for a variety of purposes in this analysis, such as evaluating electron, muon, and photon isolation variables, reconstructing jets, and computing the p_T^{miss} in the event, as described below.

The reconstructed vertex with the largest value of summed physics-object p_T^2 is the primary pp interaction vertex [26]. The physics objects are the jets, clustered using the anti- k_T jet finding algorithm [27, 28] using the tracks assigned to candidate vertices as inputs.

Electron candidates used in the selection of events for this analysis are reconstructed within $|\eta| < 2.5$ for $p_T > 25$ GeV. The electrons are also required to pass additional identification criteria: the relative amount of energy deposited in the HCAL, a match of the trajectory in the tracker with the position of the ECAL cluster [29], the number of missing measurements in the tracker, the compatibility of the electron to originate from the primary vertex, and $\sigma_{\eta\eta}$, a parameter that quantifies the spread in η of the shower in the ECAL, as discussed in Section 6. Electrons identified as arising from photon conversions are rejected [29, 30]. A high-quality ID selection is used to identify electrons in the final state, and a loose selection is used to identify electrons for vetoing events containing additional leptons.

Muons are reconstructed from information in the muon system and the tracker within $|\eta| < 2.4$ and $p_T > 20$ GeV [31]. Muon candidates must satisfy ID criteria based on the number of measurements in the muon system and the tracker, the number of matched muon-detector planes, the quality of the combined fit to the track, and the compatibility of the muon to originate from the primary vertex. A high-quality ID [31] is used to identify muons in the final state, and a loose ID [31] is used to identify muons for vetoing events with additional leptons.

Another selection on an isolation variable (Iso) is applied for both electrons and muons. Iso is defined relative to the lepton p_T by summing the p_T of the charged hadrons and neutral particles in geometrical cones of $\Delta R = \sqrt{(\Delta\eta)^2 + (\Delta\phi)^2} = 0.3$ (0.4) around the electron (muon) trajectory:

$$I^\ell = \left(\sum p_T^{\text{charged}} + \max \left[0, \sum p_T^{\text{neutral}} + \sum p_T^\gamma - p_T^{\text{PU}} \right] \right) / p_T^\ell.$$

where $\sum p_T^{\text{charged}}$ is the scalar p_T sum of charged hadrons originating from the primary vertex, and $\sum p_T^{\text{neutral}}$ and $\sum p_T^\gamma$ are, respectively, the scalar p_T sums of neutral hadrons and photons. To mitigate pileup (PU) effects, only charged hadrons originating at the primary vertex are included. For the neutral-hadron and photon components, an estimate of the expected PU contribution (p_T^{PU}) [32] is subtracted. For electrons, p_T^{PU} is evaluated using the ‘‘jet area’’ method described in Ref. [33], whereas for muons, p_T^{PU} is assumed to be one half of the scalar p_T sum deposited in the isolation cone by charged particles not associated with the primary vertex. The factor of one half corresponds to the approximate ratio of neutral to charged hadrons produced in the hadronization of PU interactions. Electrons passing the high-quality (loose) ID selection

are considered isolated if $\text{Iso} < 0.0695$ (0.175) if the pseudorapidity (η_{SC}) of the ECAL cluster is $|\eta_{\text{SC}}| < 1.479$, or $\text{Iso} < 0.0821$ (0.159) if $1.479 < |\eta_{\text{SC}}| < 2.5$. Muons are considered isolated if $\text{Iso} < 0.15$ (0.25) for the high-quality (loose) ID selection.

Photon reconstruction [34] is similar to that of electrons, and is performed in the region of $|\eta| < 2.5$ and for $p_{\text{T}} > 20$ GeV, excluding the ECAL transition region of $1.444 < |\eta| < 1.566$. To minimize photon misidentification, photon candidates must: pass an electron veto; satisfy criteria based on the distribution of energy deposited in the ECAL and HCAL; satisfy criteria on the isolation variables constructed from the kinematic inputs of the charged and neutral hadrons; and have no other photons near the photon of interest. A high-quality ID [34] is used to identify prompt photons (i.e., not originating from hadron decays) in the final state, and a loose ID [34] to identify nonprompt photons, which are mainly products of neutral pion decay.

Jets are reconstructed from PF objects using the anti- k_{T} jet clustering algorithm [27] with a distance parameter of 0.4. To reduce the contamination from PU, charged PF candidates in the tracker acceptance of $|\eta| < 2.4$ are excluded from jet clustering when they are associated with PU vertices [25]. The contribution from neutral PU particles to the jet energy is corrected based on the projected area of the jet on the front face of the calorimeter [33]. For this analysis, jets are required to have $|\eta| < 4.7$ and $p_{\text{T}} > 30$ GeV. A jet energy correction, similar to the one developed for 8 TeV collisions [35], is obtained from dedicated studies we performed on both data and simulated events (typically involving dijet, γ +jet, Z+jet, and multijet production). Other residual corrections are applied to the data as functions of p_{T} and η to correct for the small differences between data and simulation. Additional quality criteria are applied to jet candidates to remove spurious jet-like features originating from isolated noise patterns [36] in the calorimeters or the tracker.

The vector $\vec{p}_{\text{T}}^{\text{miss}}$ is computed as the negative of the vector sum of the p_{T} of all the PF candidates in an event [37], and its magnitude is denoted as $p_{\text{T}}^{\text{miss}}$. The jet energy corrections are propagated to the $\vec{p}_{\text{T}}^{\text{miss}}$. The data to simulation efficiency ratios are used as scale factors to correct the simulated event yields.

5 Event selection

Candidate events are selected by requiring exactly one electron (muon) with $p_{\text{T}} > 30$ GeV and $|\eta_{\ell}| < 2.5$ (2.4), with transverse mass of the W boson $m_{\text{T}}^{\text{W}} > 30$ GeV. We define m_{T}^{W} as $\sqrt{2p_{\text{T}}^{\ell}p_{\text{T}}^{\text{miss}}[1 - \cos(\Delta\phi_{\ell, p_{\text{T}}^{\text{miss}}})]}$, where p_{T}^{ℓ} is the p_{T} of the lepton and $\Delta\phi_{\ell, p_{\text{T}}^{\text{miss}}}$ is the azimuthal angle between the lepton and the $\vec{p}_{\text{T}}^{\text{miss}}$ directions. Events are required to contain a well-identified and isolated photon with $p_{\text{T}}^{\gamma} > 25$ GeV, $p_{\text{T}}^{\text{miss}} > 30$ GeV, and at least two jets with $|\eta| < 4.7$ and $p_{\text{T}} > 40$ (30) GeV for the leading (second) jet. To identify each candidate properly, a separation of $\Delta R > 0.5$ is required between any pair of the photon, lepton, or jets. In the electron channel we further require the invariant mass ($m_{\ell\gamma}$) of the selected photon and electron to be inconsistent with the Z boson mass peak, $|m_{\ell\gamma} - 91| > 10$ GeV, which suppresses the $Z \rightarrow e^{+}e^{-}$ background where one electron is misidentified as a photon. Based on the pseudorapidity of the photon, the electron and muon channels are each subdivided into a barrel region with $|\eta_{\gamma}| < 1.444$, and an endcap region with $1.566 < |\eta_{\gamma}| < 2.5$.

In this analysis, both a control and a signal region are defined. The control region (CR) is constructed with an aim of validating the simulated samples and background estimation methods using data. In addition to the previous selections, the control region is defined by a requirement that $200 < m_{\text{jj}} < 400$ GeV.

The signal region (SR) is defined by the previous selections plus the additional requirements that $m_{jj} > 500 \text{ GeV}$, $|\Delta\eta_{jj}| > 2.5$, $m_{W\gamma} > 100 \text{ GeV}$, $|y_{W\gamma} - (y_{j1} + y_{j2})/2| < 1.2$ [38], and $|\phi_{W\gamma} - \phi_{j1,j2}| > 2$ radians, where $m_{W\gamma}$ and $\phi_{W\gamma}$ are, respectively, the invariant mass and azimuthal angle of the W boson and γ system, $\phi_{j1,j2}$ is the azimuthal angle of the dijet system, and $y_{j1(2)}$ is the rapidity of the leading (second) jet. The longitudinal component of the neutrino momentum is estimated by solving the quadratic equation that constrains the mass of the charged lepton and neutrino system to the world-average value of the W boson mass [39]. As described in Ref. [40], when there are multiple solutions, the one with the smallest longitudinal momentum is chosen; if there are only complex solutions, the real part is chosen as the longitudinal momentum. The requirements on $|y_{W\gamma} - (y_{j1} + y_{j2})/2|$ and on $|\phi_{W\gamma} - \phi_{j1,j2}|$ are intended to ensure that the momentum of the $W\gamma$ system is balanced by that of the dijet system, which would be the case if there were no additional QCD radiation. These selection requirements were chosen by optimizing the expected significance of the EW signal.

6 Background estimation

The backgrounds in this paper are shown in Fig. 2. The largest source of background to the EW signal is QCD $W\gamma$ +jets production. The yield of this background is obtained from a simultaneous fit to the data in both the SR and CR, as described in Sections 8–10. The fit function includes constraints from the theoretical calculation of this process with its uncertainty. The treatment of additional background components is discussed in the following paragraphs.

Reconstructed photons and leptons that do not arise from outgoing particles in the hard interaction in the event are denoted as misidentified (misID) photons and leptons. This category includes physical photons and leptons, as well as those of purely instrumental origins. Because of the variety of sources of these misID particles and the difficulty of modeling instrumental effects, we use data-based methods to estimate their contribution.

The background from misID photons arises mainly from W +jets or top quark+jets events with a jet misreconstructed as a photon. The method used to estimate this background involves measuring in CMS data and applying a per-photon extrapolation factor in which the denominator is chosen to be orthogonal to the full photon selection, but similar enough that the systematic uncertainties due to the extrapolation are well understood. The photon in the denominator is required to fail the high-quality ID and pass the loose ID [8, 41]. The extrapolation factor is determined from a template fit to the photon $\sigma_{\eta\eta}$ distribution, which is small for prompt photons and large for nonprompt photons. The nonprompt template used in the fit is obtained from a sideband of the photon isolation variable in W +jets data. More details can be found in Ref. [10].

The background from jets misidentified as leptons is estimated in a similar fashion. To extrapolate from the loose leptons to the high-quality ones, an extrapolation factor is defined as:

$$\frac{f_\ell}{1 - f_\ell'}$$

where f_ℓ is the lepton misidentification rate, defined as the ratio of the number of events in the SR where the lepton passes the high-quality ID to the total number of events passing only the loose ID requirements. To reduce additional contamination from genuine leptons, the W +jets and Z +jets contributions are subtracted from both the numerator and denominator. The extrapolation factor is measured as a function of the η and p_T of the lepton in a CR dominated by dijet events. The dijet CR is defined by selecting one lepton, one jet that is well separated from the lepton, and low p_T^{miss} . This technique is also used and described in Ref. [4].

The background category “double misID” is defined as events containing both a misID photon and a misID lepton. Its yield is estimated from a sample where both the photon and the lepton that are required to pass the loose ID selection, and fail the high-quality ID. Such events are assigned a weight equal to the product of the misID extrapolation factors of the photon and lepton. Double misID events contaminate the single misID background estimate because the second object is assumed to be genuine. Consequently, each time a weight is added to the double misID estimate, the same weight is subtracted from both the single-photon and single-lepton estimates. In addition, events in which genuine photons and leptons pass the loose ID but fail the high-quality ID selection contaminate both the single and double misID estimates. This source of contamination is estimated and removed using simulated events with reconstructed objects matched to generator-level objects.

Other backgrounds, including top quark and diboson processes, are estimated from MC simulation and are normalized to the integrated luminosity of the CMS data set using inclusive cross sections calculated at NLO in QCD. The $e \rightarrow \gamma$ background includes events with an electron misID as a photon. We apply $|m_{\ell\gamma} - 91| > 10 \text{ GeV}$ to minimize this contribution. The remaining background is estimated from simulated Drell–Yan and $t\bar{t}\gamma$ events that contain a photon matched to an electron at the generator level with $\Delta R = 0.3$.

Fig. 2 shows the photon p_T distribution in the muon barrel control region for data and background estimates. The data and the estimates are in good agreement.

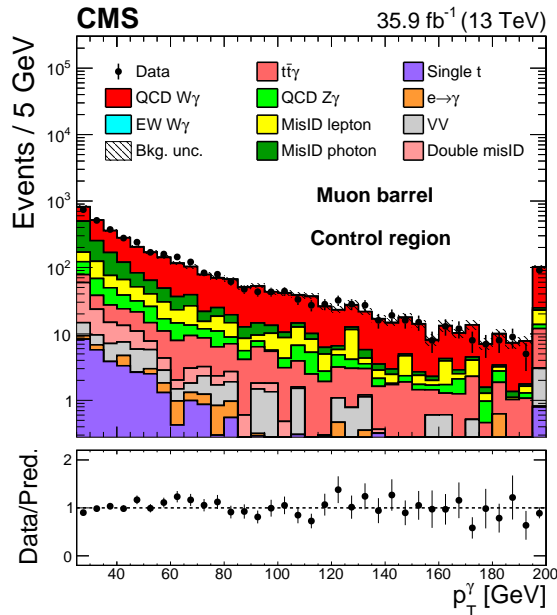


Figure 2: The photon p_T distribution in the muon barrel control region for data and background estimations. The misID backgrounds are derived from data, whereas the remaining backgrounds are estimated from simulation. All events with photon $p_T > 195 \text{ GeV}$ are included in the last bin. The hatched bands represent the total and relative statistical uncertainties on the predicted yields. The bottom graph shows the data divided by the prediction.

7 Systematic uncertainties

Systematic uncertainties that affect the measurements arise from experimental inputs, such as detector effects and the methods used to compute higher-level quantities, e.g., efficiencies, and

theoretical inputs such as the choice of the renormalization (μ_R) and factorization (μ_F) scales, and the choice of PDF sets. Each source of systematic uncertainty is quantified by evaluating its effect on the yield of the relevant signal or background categories. The uncertainties are propagated to the final distributions and calculated bin-by-bin as described in Section 8.

Table 1 summarizes all the systematic uncertainties. The systematic uncertainties in the lepton trigger, reconstruction, and selection efficiencies, measured using a tag-and-probe technique, are 2–3%. The uncertainties in jet energy scale (JES) have the largest impact on the measurement. The uncertainties in JES and jet energy resolution (JER) are calculated in simulated events by scaling and spreading the relevant observables and propagating the effects to the variables used in signal extraction and in the search for aQGC couplings. The uncertainties due to the JES and JER corresponding to different processes and different m_{jj} - $m_{\ell\gamma}$ bins are in the ranges 0.9–78% and 0.7–21%, respectively. An uncertainty of 2.5% in the integrated luminosity [42] is used for all processes estimated from simulation and for the specified fiducial cross section. The statistical uncertainties due to the finite size of both the simulated and data samples used in our background and signal prediction are estimated assuming Poisson statistics. The uncertainties related to the finite number of simulated events or to the limited number of events in the data control samples are 7–11% for the EW $W\gamma jj$ signal, 6–36% for the QCD-induced $W\gamma$ background, 43–72% for the nonprompt lepton contamination and 7–36% for the nonprompt photon background. These uncertainties are uncorrelated across different processes and bins of any single distribution, and grow with increasing m_{jj} and $m_{\ell\gamma}$.

An overall systematic uncertainty in the nonprompt photon background estimate is defined as the quadratic sum of the systematic uncertainties from several distinct sources. An uncertainty because of the choice of the isolation variable sideband is evaluated by estimating the nonprompt photon fraction with alternative choices of the isolation sideband [8]. A nonclosure uncertainty is defined by performing the nonprompt photon fraction fits using simulated events and comparing the results with the known fractions. The nonclosure uncertainty in the endcap region is worse than in the barrel region and worsens as the photon p_T increases. The overall systematic uncertainty in the nonprompt photon background is in the range of 12–22%, dominated by the nonclosure. Similarly, the dominant uncertainty in the nonprompt lepton estimate is associated with the nonclosure, which is calculated by comparing two yields, one from the γ +jets events and the other from the γ +jets events where the misID lepton rates are applied to events with a lepton that passes the loose, but fails the high-quality ID. The selection used is the same as in the main event selection, except that the m_T^W and p_T^{miss} requirements are removed to increase the statistical power. The uncertainty associated with the nonprompt lepton background is 30%.

The effects of the choice of μ_R and μ_F in the theoretical calculation for signal and background processes are estimated by independently changing μ_R and μ_F up and down by a factor of two from their nominal value in each event, with the condition that $1/2 < \mu_R/\mu_F < 2$. The uncertainties are defined as the maximal differences from the nominal values. The PDF uncertainties are evaluated according to the procedure described in Ref. [43] using the NNPDF 3.0 set. For the signal process, the scale uncertainty varies within the range of 1.5–11% and the PDF uncertainty varies within the range 3.2–5.6%, increasing with m_{jj} and $m_{\ell\gamma}$. The scale uncertainty in the QCD-induced $W\gamma$ process, which has a very large impact on the measurement, varies in the range 6.1–20%. It is constrained by the simultaneous fit to the data in the CR. The PDF uncertainty of QCD-induced $W\gamma$ production is in the range of 1–2%.

The interference term between the EW- and QCD-induced processes, i.e., $\mathcal{O}(\alpha^4\alpha_S)$ at tree level, is estimated at particle level using MG5. The contribution of the interference is calculated as

the difference between the inclusive $W\gamma jj$ production, which contains the interference term, and the sum of the pure EW- and QCD-induced $W\gamma jj$. The interference is positive, and the ratio of the interference to EW $W\gamma jj$ is in the range 2–4%, decreasing with increasing m_{jj} . These values are used as systematic uncertainties in the signal process.

A correction factor is applied to the simulated events to account for the L1 trigger occasionally firing at the wrong time because of the darkening of the ECAL crystals. This mistiming results in a loss of trigger efficiency in the data and is not modeled by the simulation. The uncertainties due to these correction factors vary by 1–4%, and are treated as correlated across different processes and bins.

Table 1: Relative systematic uncertainties in the estimated signal and background yields in units of percent. The ranges reflect the dependence of the specified uncertainty on m_{jj} and $m_{\ell\gamma}$.

Source	EW $W\gamma jj$	QCD $W\gamma jj$	VV	$t\bar{t}\gamma$	QCD $Z\gamma$	Single t	MisID photon	MisID lepton	Double misID	$e \rightarrow \gamma$
JES	0.9–6.9	11–28	6.4–38	3.7–16	12–78	3.3–18	—	—	—	11–28
JER	0.7–2.2	0.7–4.1	6.9–21	1.3–4.9	6.5–15	2.9–7.1	—	—	—	0.7–4.1
Integrated luminosity	2.5	2.5	2.5	2.5	2.5	2.5	—	—	—	2.5
MisID photon	—	—	—	—	—	—	12–22	—	12–22	—
MisID lepton	—	—	—	—	—	—	—	30	30	—
μ_R/μ_F scales	1.5–11	6.1–20	—	—	—	—	—	—	—	—
PDF	3.2–5.6	1–2	—	—	—	—	—	—	—	—
Interference	1.8–2.8	—	—	—	—	—	—	—	—	—
Cross section for $t\bar{t}\gamma$	—	—	—	10	—	—	—	—	—	—
Cross section for VV	—	—	10	—	—	—	—	—	—	—
Modeling of pileup	0–0.6	0.3–1.4	4.8–13	2.6–3.9	6.2–19	1.0–3.9	—	—	—	0.3–1.4
Statistical uncertainty	7–11	6–36	45–100	13–56	16–100	17–55	7–36	43–72	30–100	54–100
L1 mistiming	1.7–2.4	0.8–1.6	0.5–1.6	1.4–2.5	0.6–3.6	1.0–2.1	—	—	—	1.1–2.8
Muon ID/Iso	0.3	0.3	0.3	0.3	0.3	0.3	—	—	—	0.3
Muon trigger	0.3	0.2	0.2	0.2	0.1	0.1	—	—	—	0.2
Electron reconstruction	0.5	0.6	0.5	0.6	0.6	0.5	—	—	—	0.5
Electron ID/Iso	1.3	1.3	1.3	1.3	1.3	1.3	—	—	—	1.3
Electron trigger	2.5	2.5	2.5	2.5	2.5	2.5	—	—	—	2.5
Photon ID	1.2	1.2	1.1	1.2	1.3	1.2	—	—	—	1.2

All of the systematic uncertainties discussed above are applied both to the signal significance measurement and in the search for aQGC contributions. They are also propagated to the uncertainty in the measured fiducial cross section, with the exception of the theoretical uncertainties associated with the signal cross section. All of the systematic uncertainties except those that arise from the trigger efficiency and the lepton identification and misidentification are considered to be correlated between the electron and muon channels.

8 The EW $W\gamma$ production measurement

Table 2 shows the simulated signal and background yields prior to any fitting, as well as the observed data yields. To quantify the significance of the observation of EW production of the $W\gamma$ signal, we perform a statistical analysis of the event yields through a fit to the $(m_{jj}, m_{\ell\gamma})$ two-dimensional (2D) distribution. Both m_{jj} and $m_{\ell\gamma}$ are powerful variables for distinguishing between the signal and QCD $W\gamma$ background, and the 2D analysis provides a larger expected significance than either variable alone. For this measurement, and the measurements in Sections 9 and 10, the SR is further divided into four bins in m_{jj} (lower boundaries of 500, 800, 1200, and 1700 GeV) and three bins in $m_{\ell\gamma}$ (lower boundaries of 30, 80, and 130 GeV). The data in the CR are fit simultaneously with the data in the SR. Figure 3 shows the resultant 2D fitted distributions.

The signal significance is quantified on the basis of a profile likelihood test statistic [44]. This test statistic involves the ratio of two Poisson likelihood functions, one in which the signal

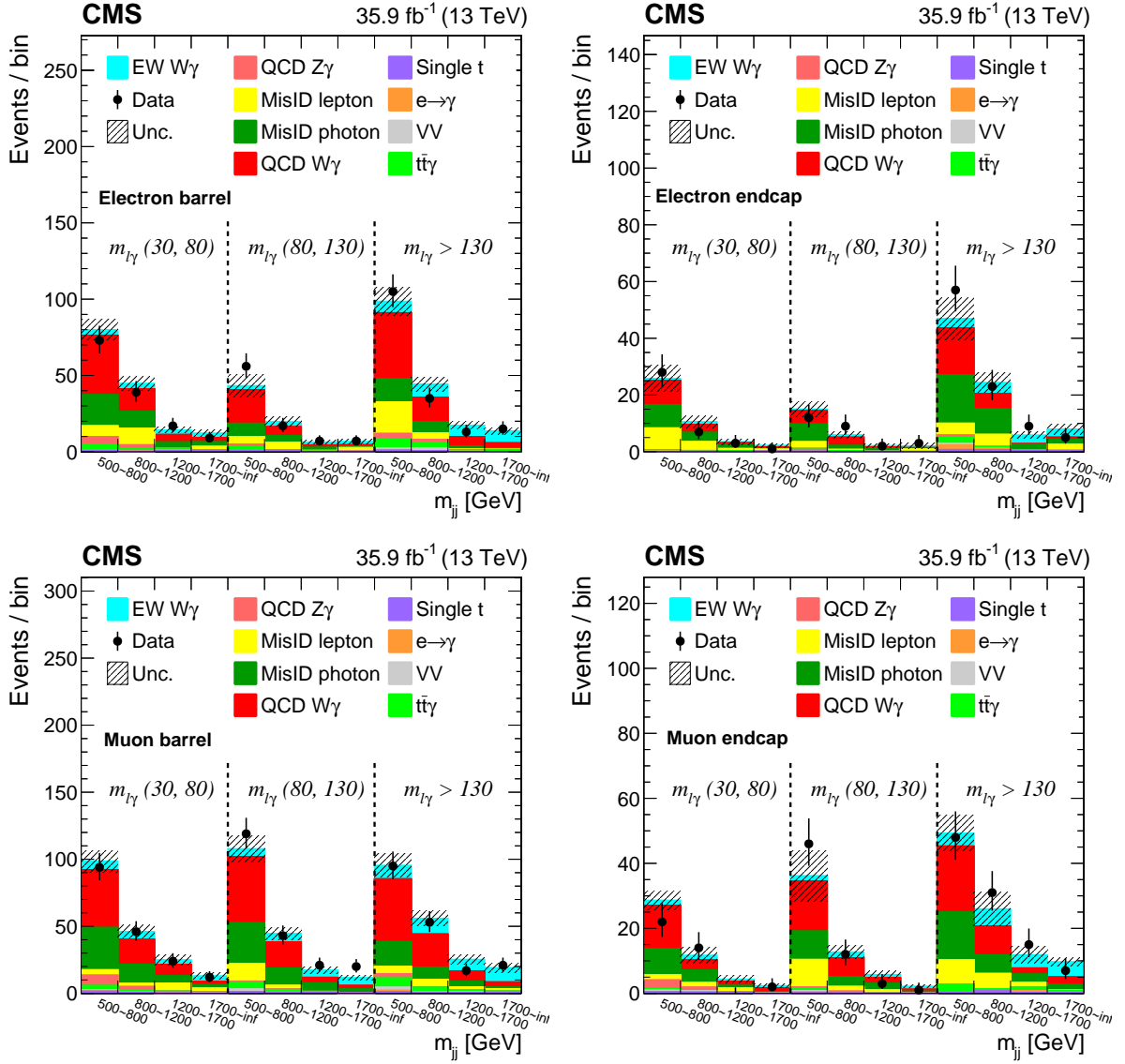


Figure 3: The 2D distributions used in the fit for the signal strength of $EW W\gamma + 2$ jets for events in the electron barrel (upper left), electron endcap (upper right), muon barrel (lower left), and muon endcap (lower right). The hatched bands represent the total and relative systematic uncertainties on the predicted yields. The predicted yields are shown with their best-fit normalizations.

Table 2: Signal, background, and data yields after the final selection. Statistical and systematic uncertainties (before the fitting) are added in quadrature.

	Electron barrel	Electron endcap	Muon barrel	Muon endcap
MisID photon	81.0 ± 5.2	48.1 ± 4.9	134.8 ± 8.2	52.1 ± 4.8
MisID lepton	63.7 ± 12.3	27.8 ± 7.2	46.8 ± 10.6	23.1 ± 6.5
QCD $W\gamma jj$	154.2 ± 12.0	41.1 ± 4.4	221.2 ± 15.8	72.1 ± 6.2
$t\bar{t}\gamma$	20.6 ± 1.6	5.1 ± 0.6	28.3 ± 1.8	6.9 ± 0.8
QCD $Z\gamma$	18.0 ± 3.1	1.9 ± 0.9	16.2 ± 3.0	4.9 ± 1.3
Single t	4.9 ± 0.8	2.5 ± 0.5	6.8 ± 0.9	2.4 ± 0.5
VV	4.2 ± 1.6	0.6 ± 0.6	7.5 ± 2.1	1.4 ± 0.7
$e \rightarrow \gamma$	1.5 ± 0.6	2.1 ± 0.8	1.7 ± 0.7	1.1 ± 0.6
Total background	348.3 ± 18.4	129.1 ± 9.9	463.4 ± 21.2	163.8 ± 10.4
EW $W\gamma jj$	48.8 ± 2.2	16.1 ± 1.0	74.5 ± 2.8	24.4 ± 1.3
Total predicted	397.1 ± 18.5	145.2 ± 10.0	537.9 ± 21.4	188.2 ± 10.5
Data	393	159	565	201

strength is fixed to zero and one in which the signal strength is allowed to have any positive value. The signal strength represents the ratio of observed to expected signal yields. Systematic uncertainties are added as parameters into the likelihood function to scale the relevant process using log-normal functions. The distribution in the test statistic is assumed to be in the asymptotic regime where there is a simple relationship between its value and the significance of the result [45]. The observed (expected) signal strength parameter is $\hat{\mu} = 1.20_{-0.24}^{+0.26}$ ($1.00_{-0.25}^{+0.27}$), corresponding to an observed (expected) statistical significance of 4.9 (4.6) SD for the analyzed 13 TeV data set.

This result can be combined with the previous CMS measurement at 8 TeV described in Ref. [9] assuming the signal strength does not change with the center of mass energy. There are two uncertainties that are correlated between the 8 and 13 TeV analyses. The theoretical uncertainties in the signal and QCD $W\gamma$ background of the 8 TeV analysis include multiple sources, but are dominated by the renormalization and factorization scale uncertainties, and are therefore correlated with the corresponding uncertainties in the 13 TeV analysis. All other uncertainties are uncorrelated between the 8 and 13 TeV analyses. After combining our result with that at 8 TeV using this correlation scheme, the observed (expected) significance is 5.3 (4.8) SD.

9 Fiducial EW $W\gamma jj$ cross section measurement

A fiducial cross section at 13 TeV is extracted in the same m_{jj} - $m_{\ell\gamma}$ binning used in the calculation of significance, and through the same simultaneous fit used in the CR. The fiducial region is defined using the MC generator quantities: one lepton with $p_T^\ell > 30$ GeV and $|\eta_\ell| < 2.4$, $p_T^{\text{miss}} > 30$ GeV, $p_T^\gamma > 25$ GeV, $|\eta_\gamma| < 1.444$ or $1.566 < |\eta_\gamma| < 2.5$, $m_T^W > 30$ GeV, two jets with $p_T^{j(2)} > 40$ (30) GeV, with $|\eta_j| < 4.7$, $m_{jj} > 500$ GeV, and $|\Delta\eta_{jj}| > 2.5$. The leptons are reconstructed at the particle level with fully recovered final-state radiation. The acceptance is defined as the fraction of the generated signal events passing the fiducial region selection, which is extracted using MG5. The theoretical uncertainty because of the extrapolation between the fiducial and SR is negligible ($< 1\%$). We define the cross section as

$$\sigma^{\text{fid}}(13 \text{ TeV}) = \sigma_g \hat{\mu} \alpha_{gf},$$

where the cross section for the generated signal events is $\sigma_g = 0.776$ pb, the signal strength parameter $\hat{\mu} = 1.20^{+0.26}_{-0.24}$, and the acceptance $\alpha_{gf} = 0.02195$. The observed fiducial cross section is $\sigma_{EW}^{\text{fid}}(13 \text{ TeV}) = 20.4 \pm 0.4$ (lumi) ± 2.8 (stat) ± 3.5 (syst) fb = 20.4 ± 4.5 fb.

10 Fiducial EW+QCD $W\gamma jj$ cross section measurement

In addition to the EW $W\gamma jj$ process, we also determine a cross section for inclusive EW+QCD $W\gamma jj$ production. The fiducial region is the same as that for EW $W\gamma jj$ and the formula for the cross section is

$$\sigma^{\text{fid}} = \mu \left\{ \sigma_g^{\text{EW}} \alpha_{gf}^{\text{EW}} + \sigma_g^{\text{QCD}} \alpha_{gf}^{\text{QCD}} \right\}.$$

Since the QCD $W\gamma+2$ jets is part of the signal, the CR is no longer included in the calculated signal strength.

The inputs used for the fit are similar to the ones for EW $W\gamma jj$, with the difference that EW and QCD $W\gamma jj$ are combined as signal. The cross section for QCD $W\gamma jj$ is 178.6 pb, and α_{gf}^{QCD} is calculated to be 0.0004068. The measured signal strength for inclusive $W\gamma jj$ is $1.21^{+0.17}_{-0.16}$ and the observed fiducial cross section is $\sigma_{EW+QCD}^{\text{fid}}(13 \text{ TeV}) = 108 \pm 2$ (lumi) ± 5 (stat) ± 15 (syst) fb = 108 ± 16 fb. Figure 4 shows the post-fit results.

11 Limits on anomalous quartic gauge couplings

The effects of BSM physics can be modeled in a generic way through a collection of linearly independent higher-dimensional operators in effective field theory [11]. As mentioned above, VBS is more suitable to constrain aQGC. The lowest dimension operators that modify quartic gauge couplings but do not exhibit two or three weak gauge boson vertices are dimension-eight. Reference [46] proposes nine independent charge-conjugate and parity-conserving dimension-eight effective operators by assuming the $SU(2) \times U(1)$ symmetry of the EW gauge field. The model includes a Higgs doublet to incorporate the presence of an SM Higgs boson. A contribution from aQGCs enhances the production of events with large $W\gamma$ mass. The operators affecting the $W\gamma jj$ channel can be divided into two categories. The operators $\mathcal{L}_{M,0} - \mathcal{L}_{M,7}$ contain an $SU(2)$ field strength, the $U(1)$ field strength, and the covariant derivative of the Higgs doublet field. The operators $\mathcal{L}_{T,0} - \mathcal{L}_{T,2}$ and $\mathcal{L}_{T,5} - \mathcal{L}_{T,7}$, contain only the two field strengths. The coefficient of the operator $\mathcal{L}_{X,Y}$ is denoted by $f_{X,Y}/\Lambda^4$, where Λ is the unknown scale of BSM physics.

A simulation is performed that includes the effects of the aQGCs in addition to the SM EW $W\gamma jj$ process, as well as any interference between the two. We use the $m_{W\gamma}$ distribution to extract limits on the aQGC parameters. To obtain a continuous prediction for the signal as a function of the anomalous coupling, a quadratic fit is performed to a SM+aQGC yield as a function of the aQGC coefficient, separately in each $m_{W\gamma}$ bin in the aQGC region, which is defined based on the common selection in Section 5, with the further requirements $m_{jj} > 800$ GeV, $|\Delta\eta_{jj}| > 2.5$, $m_{W\gamma} > 150$ GeV, and $p_T^\gamma > 100$ GeV.

Figure 5 shows the resulting distribution in $m_{W\gamma}$. No statistically significant excess of events relative to the SM prediction is observed.

The following profile likelihood test statistic is used in the aQGC limit setting procedure:

$$t_{\alpha_{\text{test}}} = -2 \log \frac{\mathcal{L}(\alpha_{\text{test}}, \hat{\theta})}{\mathcal{L}(\hat{\alpha}, \hat{\theta})}.$$

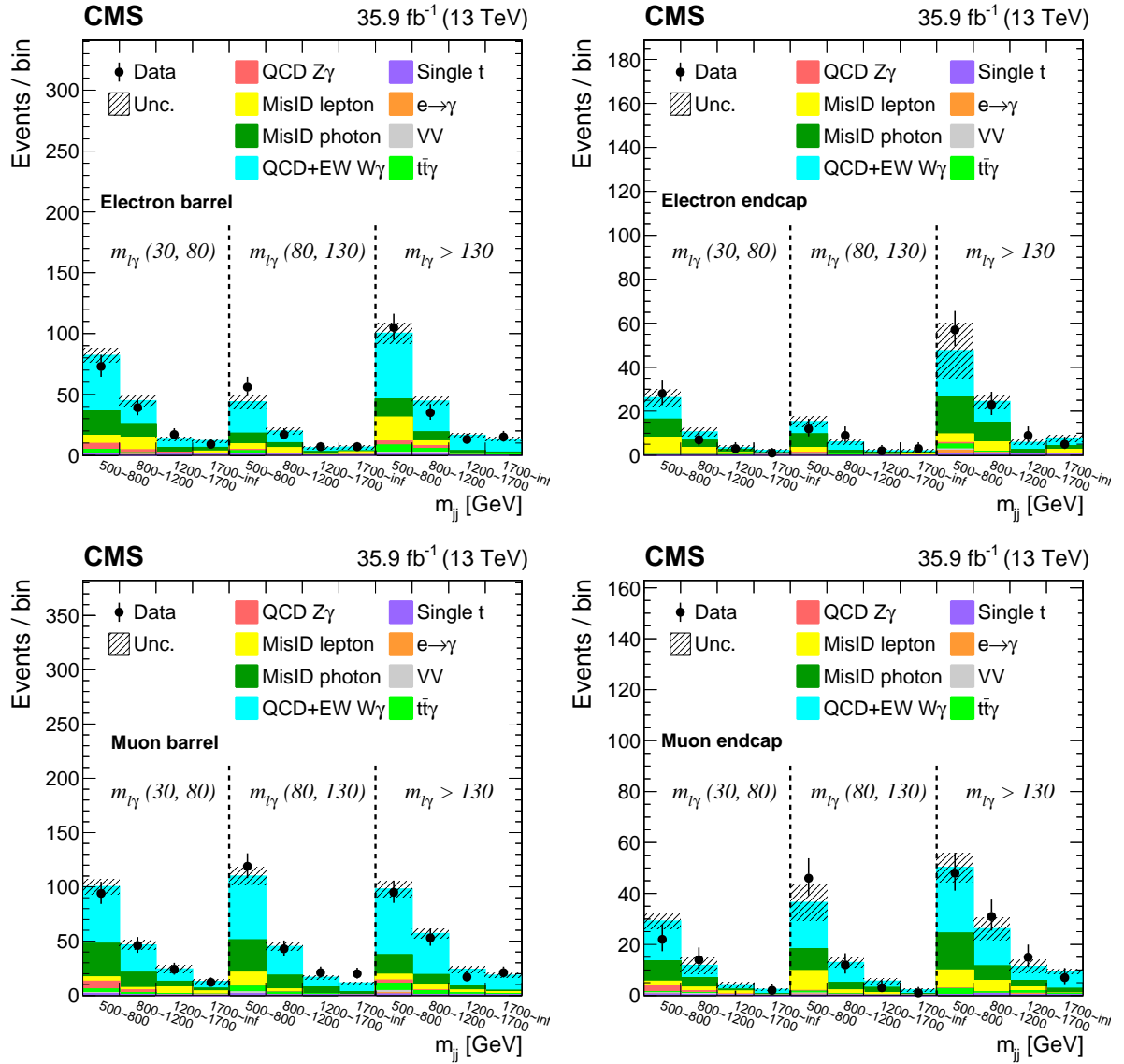


Figure 4: The 2D distributions used in the fit for the signal strength of EW+QCD $W\gamma+2$ jets in the electron barrel (upper left), electron endcap (upper right), muon barrel (lower left) and muon endcap (lower right). The hatched bands represent the total and relative systematic uncertainties on the predicted yields. The predicted yields are shown with their best-fit normalizations.

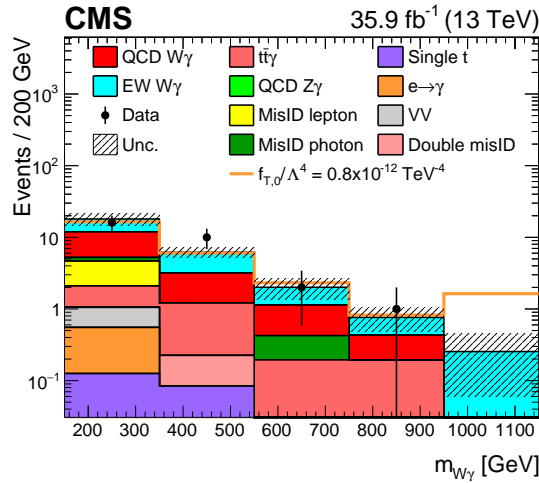


Figure 5: The $m_{W\gamma}$ distribution of events satisfying the aQGC region selection, which is used to set constraints on the anomalous coupling parameters. The orange line represents a nonzero $f_{T,0}/\Lambda^4$ setting. All events with $m_{W\gamma} > 950$ GeV are included in the last bin. The hatched bands represent the total and relative statistical uncertainties in the predicted yields.

The likelihood function is the product of Poisson distributions and a normal constraining term with nuisance parameters representing the sources of systematic uncertainties in each bin. The final likelihood function is the product of the likelihood functions of the electron and muon channels. The main constraint on the aQGC parameters is from the highest $m_{W\gamma}$ bin. The parameter α_{test} represents the aQGC point being tested, and the symbol θ represents a vector of nuisance parameters assumed to follow log-normal distributions. The parameter $\hat{\theta}$ corresponds to the maximum of the likelihood function at the point α_{test} . The $\hat{\alpha}$ and $\hat{\theta}$ parameters correspond to the single global maximum of the likelihood function. This test statistic is assumed to follow a noncentral χ^2 distribution [44]. It is therefore possible to extract the limits immediately from the difference in the negative log-likelihood (NLL) function $\Delta\text{NLL} = t_{\alpha_{\text{test}}}/2$ [47]. The 95% confidence level (CL) limit on a one-dimensional aQGC parameter corresponds to $2\Delta\text{NLL} = 3.84$. Figure 6 shows the likelihood scan of parameter $f_{T,0}/\Lambda^4$ in the calculation of the observed limits.

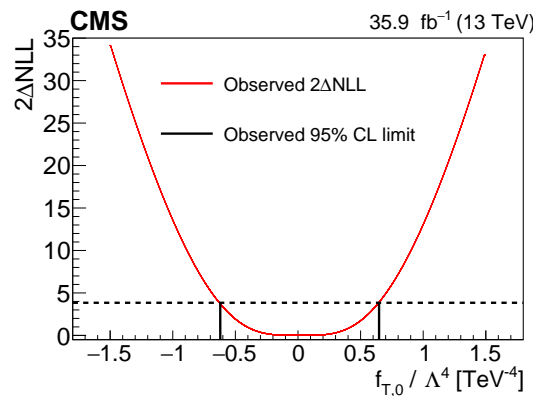


Figure 6: Observed 95% CL interval on the aQGC parameter $f_{T,0}/\Lambda^4$.

The observed and expected 95% CL limits on the coefficients of these operators, shown in Table 3, are obtained by varying the coefficient of one operator at a time, with all others set to 0, the corresponding SM value. The yield of the EW signal in any bin is a quadratic function of the coefficient, whose minimum in general does not occur at a coefficient value of 0 because

of interference with the SM operators. We therefore set upper and lower limits on the operator coefficients through a limit-setting procedure that involves first obtaining the global maximum of the profile likelihood function, and then the maximum of the profile likelihood function at fixed coefficient values, which can be compared to the global maximum and converted to CLs. The unitarity bound (U_{bound}) is defined as the scattering energy at which the aQGC coupling strength, when set equal to the observed limit, would result in a scattering amplitude that violates unitarity. The value of U_{bound} is determined using the VBFNLO 2.7.1 framework [48], taking into account the difference between VBFNLO and MG5. These are the most stringent limits to date on the aQGC parameters $f_{M,2-5}/\Lambda^4$ and $f_{T,6-7}/\Lambda^4$.

Table 3: The exclusion limits at 95% CL on each aQGC coefficient, parameterized using the distribution in $m_{W\gamma}$, and listed along with the unitarity bound. All coupling parameter limits are in TeV^{-4} , while the U_{bound} values are in TeV.

Parameters	Exp. limit	Obs. limit	U_{bound}
$f_{M,0}/\Lambda^4$	[-8.1, 8.0]	[-7.7, 7.6]	1.0
$f_{M,1}/\Lambda^4$	[-12, 12]	[-11, 11]	1.2
$f_{M,2}/\Lambda^4$	[-2.8, 2.8]	[-2.7, 2.7]	1.3
$f_{M,3}/\Lambda^4$	[-4.4, 4.4]	[-4.0, 4.1]	1.5
$f_{M,4}/\Lambda^4$	[-5.0, 5.0]	[-4.7, 4.7]	1.5
$f_{M,5}/\Lambda^4$	[-8.3, 8.3]	[-7.9, 7.7]	1.8
$f_{M,6}/\Lambda^4$	[-16, 16]	[-15, 15]	1.0
$f_{M,7}/\Lambda^4$	[-21, 20]	[-19, 19]	1.3
$f_{M,0}/\Lambda^4$	[-0.6, 0.6]	[-0.6, 0.6]	1.4
$f_{M,1}/\Lambda^4$	[-0.4, 0.4]	[-0.3, 0.4]	1.5
$f_{M,2}/\Lambda^4$	[-1.0, 1.2]	[-1.0, 1.2]	1.5
$f_{M,5}/\Lambda^4$	[-0.5, 0.5]	[-0.4, 0.4]	1.8
$f_{M,6}/\Lambda^4$	[-0.4, 0.4]	[-0.3, 0.4]	1.7
$f_{M,7}/\Lambda^4$	[-0.9, 0.9]	[-0.8, 0.9]	1.8

12 Summary

The cross section for the electroweak production of a W boson, a photon, and two jets is measured in proton-proton collisions at a center-of-mass energy of 13 TeV. The data correspond to an integrated luminosity of 35.9 fb^{-1} collected with the CMS detector. Events are selected by requiring one identified lepton (electron or muon), a moderate missing transverse momentum, one photon, and two jets with a large rapidity separation and a large dijet mass. The observed significance is 4.9 standard deviations, where a significance of 4.6 standard deviations is expected based on the standard model. After combination with previously reported CMS results based on 8 TeV data, the observed (expected) signal significance is 5.3 (4.8) standard deviations. This constitutes the first observation of electroweak $W\gamma jj$ production in proton-proton collisions. The cross section for the electroweak $W\gamma jj$ production in a restricted fiducial region is measured as $20.4 \pm 4.5 \text{ fb}$ and the total cross section for $W\gamma$ production in association with 2 jets in the same fiducial region is $108 \pm 16 \text{ fb}$, consistent with standard model predictions. Constraints placed on anomalous quartic gauge couplings in terms of dimension-8 effective field theory operators are competitive with previous results. For the parameters $f_{M,2-5}/\Lambda^4$ and $f_{T,6-7}/\Lambda^4$, the constraints are the most stringent to date.

Acknowledgments

We congratulate our colleagues in the CERN accelerator departments for the excellent performance of the LHC and thank the technical and administrative staffs at CERN and at other CMS institutes for their contributions to the success of the CMS effort. In addition, we gratefully acknowledge the computing centers and personnel of the Worldwide LHC Computing Grid for delivering so effectively the computing infrastructure essential to our analyses. Finally, we acknowledge the enduring support for the construction and operation of the LHC and the CMS detector provided by the following funding agencies: BMBWF and FWF (Austria); FNRS and FWO (Belgium); CNPq, CAPES, FAPERJ, FAPERGS, and FAPESP (Brazil); MES (Bulgaria); CERN; CAS, MoST, and NSFC (China); COLCIENCIAS (Colombia); MSES and CSF (Croatia); RIF (Cyprus); SENESCYT (Ecuador); MoER, ERC IUT, PUT and ERDF (Estonia); Academy of Finland, MEC, and HIP (Finland); CEA and CNRS/IN2P3 (France); BMBF, DFG, and HGF (Germany); GSRT (Greece); NKFI (Hungary); DAE and DST (India); IPM (Iran); SFI (Ireland); INFN (Italy); MSIP and NRF (Republic of Korea); MES (Latvia); LAS (Lithuania); MOE and UM (Malaysia); BUAP, CINVESTAV, CONACYT, LNS, SEP, and UASLP-FAI (Mexico); MOS (Montenegro); MBIE (New Zealand); PAEC (Pakistan); MSHE and NSC (Poland); FCT (Portugal); JINR (Dubna); MON, RosAtom, RAS, RFBR, and NRC KI (Russia); MESTD (Serbia); SEIDI, CPAN, PCTI, and FEDER (Spain); MOSTR (Sri Lanka); Swiss Funding Agencies (Switzerland); MST (Taipei); ThEPCenter, IPST, STAR, and NSTDA (Thailand); TUBITAK and TAEK (Turkey); NASU (Ukraine); STFC (United Kingdom); DOE and NSF (USA).

Individuals have received support from the Marie-Curie program and the European Research Council and Horizon 2020 Grant, contract Nos. 675440, 752730, and 765710 (European Union); the Leventis Foundation; the A.P. Sloan Foundation; the Alexander von Humboldt Foundation; the Belgian Federal Science Policy Office; the Fonds pour la Formation à la Recherche dans l'Industrie et dans l'Agriculture (FRIA-Belgium); the Agentschap voor Innovatie door Wetenschap en Technologie (IWT-Belgium); the F.R.S.-FNRS and FWO (Belgium) under the "Excellence of Science – EOS" – be.h project n. 30820817; the Beijing Municipal Science & Technology Commission, No. Z191100007219010; the Ministry of Education, Youth and Sports (MEYS) of the Czech Republic; the Deutsche Forschungsgemeinschaft (DFG) under Germany's Excellence Strategy – EXC 2121 "Quantum Universe" – 390833306; the Lendület ("Momentum") Program and the János Bolyai Research Scholarship of the Hungarian Academy of Sciences, the New National Excellence Program ÚNKP, the NKFI research grants 123842, 123959, 124845, 124850, 125105, 128713, 128786, and 129058 (Hungary); the Council of Science and Industrial Research, India; the HOMING PLUS program of the Foundation for Polish Science, cofinanced from European Union, Regional Development Fund, the Mobility Plus program of the Ministry of Science and Higher Education, the National Science Center (Poland), contracts Harmonia 2014/14/M/ST2/00428, Opus 2014/13/B/ST2/02543, 2014/15/B/ST2/03998, and 2015/19/B/ST2/02861, Sonata-bis 2012/07/E/ST2/01406; the National Priorities Research Program by Qatar National Research Fund; the Ministry of Science and Higher Education, project no. 02.a03.21.0005 (Russia); the Programa Estatal de Fomento de la Investigación Científica y Técnica de Excelencia María de Maeztu, grant MDM-2015-0509 and the Programa Severo Ochoa del Principado de Asturias; the Thalís and Aristeia programs cofinanced by EU-ESF and the Greek NSRF; the Rachadapisek Sompot Fund for Postdoctoral Fellowship, Chulalongkorn University and the Chulalongkorn Academic into Its 2nd Century Project Advancement Project (Thailand); the Kavli Foundation; the Nvidia Corporation; the SuperMicro Corporation; the Welch Foundation, contract C-1845; and the Weston Havens Foundation (USA).

References

- [1] ATLAS Collaboration, “Observation of a new particle in the search for the standard model Higgs boson with the ATLAS detector at the LHC”, *Phys. Lett. B* **716** (2012) 1, doi:10.1016/j.physletb.2012.08.020, arXiv:1207.7214.
- [2] CMS Collaboration, “Observation of a new boson at a mass of 125 GeV with the CMS experiment at the LHC”, *Phys. Lett. B* **716** (2012) 30, doi:10.1016/j.physletb.2012.08.021, arXiv:1207.7235.
- [3] CMS Collaboration, “Observation of a new boson with mass near 125 GeV in pp collisions at $\sqrt{s} = 7$ and 8 TeV”, *JHEP* **06** (2013) 081, doi:10.1007/jhep06(2013)081, arXiv:1303.4571.
- [4] CMS Collaboration, “Observation of electroweak production of same-sign W boson pairs in the two jet and two same-sign lepton final state in proton-proton collisions at $\sqrt{s} = 13$ TeV”, *Phys. Rev. Lett.* **120** (2018) 081801, doi:10.1103/PhysRevLett.120.081801, arXiv:1709.05822.
- [5] ATLAS Collaboration, “Observation of electroweak production of a same-sign W boson pair in association with two jets in pp collisions at $\sqrt{s} = 13$ TeV with the ATLAS detector”, *Phys. Rev. Lett.* **123** (2019) 161801, doi:10.1103/physrevlett.123.161801, arXiv:1906.03203.
- [6] CMS Collaboration, “Measurements of production cross sections of WZ and same-sign WW boson pairs in association with two jets in proton-proton collisions at $\sqrt{s} = 13$ TeV”, (2020). arXiv:2005.01173. Submitted to *Phys. Lett. B*.
- [7] ATLAS Collaboration, “Studies of $Z\gamma$ production in association with a high-mass dijet system in pp collisions at $\sqrt{s} = 8$ TeV with the ATLAS detector”, *JHEP* **07** (2017) 107, doi:10.1007/JHEP07(2017)107, arXiv:1705.01966.
- [8] CMS Collaboration, “Measurement of the cross section for electroweak production of $Z\gamma$ in association with two jets and constraints on anomalous quartic gauge couplings in proton-proton collisions at $\sqrt{s} = 8$ TeV”, *Phys. Lett. B* **770** (2017) 380, doi:10.1016/j.physletb.2017.04.071, arXiv:1702.03025.
- [9] CMS Collaboration, “Measurement of electroweak-induced production of $W\gamma$ with two jets in pp collisions at $\sqrt{s} = 8$ TeV and constraints on anomalous quartic gauge couplings”, *JHEP* **06** (2017) 106, doi:10.1007/JHEP06(2017)106, arXiv:1612.09256.
- [10] CMS Collaboration, “Measurement of the cross section for electroweak production of a Z boson, a photon and two jets in proton-proton collisions at $\sqrt{s} = 13$ TeV and constraints on anomalous quartic couplings”, *Journal of High Energy Physics* **06** (2020) 076, doi:10.1007/jhep06(2020)076, arXiv:2002.09902.
- [11] C. Degrande et al., “Effective field theory: A modern approach to anomalous couplings”, *Ann. Phys.* **335** (2013) 21, doi:10.1016/j.aop.2013.04.016, arXiv:1205.4231.
- [12] CMS Collaboration, “The CMS experiment at the CERN LHC”, *JINST* **3** (2008) S08004, doi:10.1088/1748-0221/3/08/S08004.

- [13] V. A. Khoze, M. G. Ryskin, W. J. Stirling, and P. H. Williams, “A Z-monitor to calibrate Higgs production via vector boson fusion with rapidity gaps at the LHC”, *Eur. Phys. J. C* **26** (2003) 429, doi:10.1140/epjc/s2002-01069-2, arXiv:hep-ph/0207365.
- [14] C. Oleari and D. Zeppenfeld, “QCD corrections to electroweak $\ell\nu jj$ and $\ell^+\ell^-jj$ production”, *Phys. Rev. D* **69** (2004) 093004, doi:10.1103/PhysRevD.69.093004, arXiv:hep-ph/0310156.
- [15] CMS Collaboration, “The CMS trigger system”, *JINST* **12** (2017) P01020, doi:10.1088/1748-0221/12/01/P01020, arXiv:1609.02366.
- [16] J. Alwall et al., “The automated computation of tree-level and next-to-leading order differential cross sections, and their matching to parton shower simulations”, *JHEP* **07** (2014) 079, doi:10.1007/JHEP07(2014)079, arXiv:1405.0301.
- [17] R. Frederix and S. Frixione, “Merging meets matching in MC@NLO”, *JHEP* **12** (2012) 061, doi:10.1007/JHEP12(2012)061, arXiv:1209.6215.
- [18] T. Sjöstrand et al., “An introduction to PYTHIA 8.2”, *Comput. Phys. Commun.* **191** (2015) 159, doi:10.1016/j.cpc.2015.01.024, arXiv:1410.3012.
- [19] S. Alioli, P. Nason, C. Oleari, and E. Re, “A general framework for implementing NLO calculations in shower Monte Carlo programs: the POWHEG BOX”, *JHEP* **06** (2010) 043, doi:10.1007/JHEP06(2010)043, arXiv:1002.2581.
- [20] P. Skands, S. Carrazza, and J. Rojo, “Tuning PYTHIA 8.1: the Monash 2013 tune”, *Eur. Phys. J. C* **74** (2014) 3024, doi:10.1140/epjc/s10052-014-3024-y, arXiv:1404.5630.
- [21] CMS Collaboration, “Event generator tunes obtained from underlying event and multiparton scattering measurements”, *Eur. Phys. J. C* **76** (2016) 155, doi:10.1140/epjc/s10052-016-3988-x, arXiv:1512.00815.
- [22] NNPDF Collaboration, “Parton distributions for the LHC Run II”, *JHEP* **04** (2015) 040, doi:10.1007/JHEP04(2015)040, arXiv:1410.8849.
- [23] GEANT4 Collaboration, “GEANT4 — a simulation toolkit”, *Nucl. Instrum. Meth. A* **506** (2003) 250, doi:10.1016/S0168-9002(03)01368-8.
- [24] CMS Collaboration, “Measurement of the inclusive W and Z production cross sections in pp collisions at $\sqrt{s} = 13$ TeV”, *JHEP* **10** (2011) 132, doi:10.1007/JHEP10(2011)132, arXiv:1107.4789.
- [25] CMS Collaboration, “Particle-flow reconstruction and global event description with the CMS detector”, *JINST* **12** (2017) P10003, doi:10.1088/1748-0221/12/10/P10003, arXiv:1706.04965.
- [26] CMS Collaboration, “Description and performance of track and primary-vertex reconstruction with the CMS tracker”, *JINST* **9** (2014) P10009, doi:10.1088/1748-0221/9/10/P10009, arXiv:1405.6569.
- [27] M. Cacciari, G. P. Salam, and G. Soyez, “The anti- k_T jet clustering algorithm”, *JHEP* **04** (2008) 063, doi:10.1088/1126-6708/2008/04/063, arXiv:0802.1189.

-
- [28] M. Cacciari, G. P. Salam, and G. Soyez, “FastJet user manual”, *Eur. Phys. J. C* **72** (2012) 1896, doi:10.1140/epjc/s10052-012-1896-2, arXiv:1111.6097.
- [29] CMS Collaboration, “Performance of electron reconstruction and selection with the CMS detector in proton-proton collisions at $\sqrt{s} = 8$ TeV”, *JINST* **10** (2015) P06005, doi:10.1088/1748-0221/10/06/P06005, arXiv:1502.02701.
- [30] CMS Collaboration, “Energy calibration and resolution of the CMS electromagnetic calorimeter in pp collision at $\sqrt{s} = 7$ TeV”, *JINST* **8** (2013) P09009, doi:10.1088/1748-0221/8/09/P09009, arXiv:1306.2016.
- [31] CMS Collaboration, “Performance of the CMS muon detector and muon reconstruction with proton-proton collisions at $\sqrt{s} = 13$ TeV”, *JINST* **13** (2018) P06015, doi:10.1088/1748-0221/13/06/p06015, arXiv:1804.04528.
- [32] CMS Collaboration, “Performance of the reconstruction and identification of high-momentum muons in proton-proton collisions at $\sqrt{s} = 13$ TeV”, *JINST* **15** (2020) P02027, doi:10.1088/1748-0221/15/02/p02027, arXiv:1912.03516.
- [33] M. Cacciari and G. P. Salam, “Pileup subtraction using jet areas”, *Phys. Lett. B* **659** (2008) 119, doi:10.1016/j.physletb.2007.09.077, arXiv:0707.1378.
- [34] CMS Collaboration, “Performance of photon reconstruction and identification with the CMS detector in proton-proton collisions at $\sqrt{s} = 8$ TeV”, *JINST* **10** (2015) P08010, doi:10.1088/1748-0221/10/08/P08010, arXiv:1502.02702.
- [35] CMS Collaboration, “Determination of jet energy calibration and transverse momentum resolution in CMS”, *JINST* **6** (2011) P11002, doi:10.1088/1748-0221/6/11/P11002, arXiv:1107.4277.
- [36] CMS Collaboration, “Jet performance in pp collisions at $\sqrt{s} = 7$ TeV”, CMS Physics Analysis Summary CMS-PAS-JME-10-003, CERN Geneva 2010.
- [37] CMS Collaboration, “Performance of missing transverse momentum reconstruction in proton-proton collisions at $\sqrt{s} = 13$ TeV using the CMS detector”, *JINST* **14** (2019) P07004, doi:10.1088/1748-0221/14/07/P07004, arXiv:1903.06078.
- [38] D. Rainwater, R. Szalapski, and D. Zeppenfeld, “Probing color singlet exchange in Z+2-jet events at the CERN LHC”, *Phys. Rev. D* **54** (1996) 6680, doi:10.1103/PhysRevD.54.6680, arXiv:hep-ph/9605444.
- [39] Particle Data Group, M. Tanabashi et al., “Review of particle physics”, *Phys. Rev. D* **98** (2018) 030001, doi:10.1103/PhysRevD.98.030001.
- [40] CMS Collaboration, “Search for a heavy resonance decaying to a pair of vector bosons in the lepton plus merged jet final state at $\sqrt{s} = 13$ TeV”, *JHEP* **05** (2018) 088, doi:10.1007/JHEP05(2018)088, arXiv:1802.09407.
- [41] CMS Collaboration, “Measurement of $W\gamma$ and $Z\gamma$ production in pp collisions at $\sqrt{s} = 7$ TeV”, *Phys. Lett. B* **701** (2011) 535, doi:10.1016/j.physletb.2011.06.034, arXiv:1105.2758.
- [42] CMS Collaboration, “CMS luminosity measurements for the 2016 data-taking period”, CMS Physics Analysis Summary CMS-PAS-LUM-17-001, CERN Geneva 2017.

- [43] J. Butterworth et al., “PDF4LHC recommendations for LHC Run II”, *J. Phys. G* **43** (2016) 023001, doi:10.1088/0954-3899/43/2/023001, arXiv:1510.03865.
- [44] S. S. Wilks, “The large-sample distribution of the likelihood ratio for testing composite hypotheses”, *Ann. Math. Statist.* **9** (1938) 60, doi:10.1214/aoms/1177732360.
- [45] G. Cowan, K. Cranmer, E. Gross, and O. Vitells, “Asymptotic formulae for likelihood-based tests of new physics”, *Eur. Phys. J. C* **71** (2011) 1554, doi:10.1140/epjc/s10052-011-1554-0, arXiv:1007.1727. [Erratum: doi:10.1140/epjc/s10052-013-2501-z].
- [46] O. J. P. Éboli, M. C. Gonzalez-Garcia, and J. K. Mizukoshi, “ $pp \rightarrow jje^\pm \mu^\pm \nu \nu$ and $jje^\pm \mu^\mp \nu \nu$ at $\mathcal{O}(\alpha_{\text{em}}^6)$ and $\mathcal{O}(\alpha_{\text{em}}^4 \alpha_s^2)$ for the study of the quartic electroweak gauge boson vertex at CERN LHC”, *Phys. Rev. D* **74** (2006) 073005, doi:10.1103/PhysRevD.74.073005, arXiv:hep-ph/0606118.
- [47] CMS Collaboration, “Precise determination of the mass of the Higgs boson and tests of compatibility of its couplings with the standard model predictions using proton collisions at 7 and 8 TeV”, *Eur. Phys. J. C* **75** (2014) 212, doi:10.1140/epjc/s10052-015-3351-7, arXiv:1412.8662.
- [48] K. Arnold et al., “VBFNLO: A parton level Monte Carlo for processes with electroweak bosons”, *Comput. Phys. Commun.* **180** (2009) 1661, doi:10.1016/j.cpc.2009.03.006, arXiv:0811.4559.

A The CMS Collaboration

Yerevan Physics Institute, Yerevan, Armenia

A.M. Sirunyan[†], A. Tumasyan

Institut für Hochenergiephysik, Wien, Austria

W. Adam, F. Ambrogio, T. Bergauer, M. Dragicevic, J. Erö, A. Escalante Del Valle, R. Frühwirth¹, M. Jeitler¹, N. Krammer, L. Lechner, D. Liko, T. Madlener, I. Mikulec, F.M. Pitters, N. Rad, J. Schieck¹, R. Schöfbeck, M. Spanring, S. Templ, W. Waltenberger, C.-E. Wulz¹, M. Zarucki

Institute for Nuclear Problems, Minsk, Belarus

V. Chekhovskiy, A. Litomin, V. Makarenko, J. Suarez Gonzalez

Universiteit Antwerpen, Antwerpen, Belgium

M.R. Darwish², E.A. De Wolf, D. Di Croce, X. Janssen, T. Kello³, A. Lelek, M. Pieters, H. Rejeb Sfar, H. Van Haevermaet, P. Van Mechelen, S. Van Putte, N. Van Remortel

Vrije Universiteit Brussel, Brussel, Belgium

F. Blekman, E.S. Bols, S.S. Chhibra, J. D'Hondt, J. De Clercq, D. Lontkovskiy, S. Lowette, I. Marchesini, S. Moortgat, A. Morton, Q. Python, S. Tavernier, W. Van Doninck, P. Van Mulders

Université Libre de Bruxelles, Bruxelles, Belgium

D. Beghin, B. Bilin, B. Clerboux, G. De Lentdecker, B. Dorney, L. Favart, A. Grebenyuk, A.K. Kalsi, I. Makarenko, L. Moureaux, L. Pétré, A. Popov, N. Postiau, E. Starling, L. Thomas, C. Vander Velde, P. Vanlaer, D. Vannerom, L. Wezenbeek

Ghent University, Ghent, Belgium

T. Cornelis, D. Dobur, M. Gruchala, I. Khvastunov⁴, M. Niedziela, C. Roskas, K. Skovpen, M. Tytgat, W. Verbeke, B. Vermassen, M. Vit

Université Catholique de Louvain, Louvain-la-Neuve, Belgium

G. Bruno, F. Bury, C. Caputo, P. David, C. Delaere, M. Delcourt, I.S. Donertas, A. Giammanco, V. Lemaitre, K. Mondal, J. Prisciandaro, A. Taliencio, M. Teklishyn, P. Vischia, S. Wuyckens, J. Zobec

Centro Brasileiro de Pesquisas Físicas, Rio de Janeiro, Brazil

G.A. Alves, G. Correia Silva, C. Hensel, A. Moraes

Universidade do Estado do Rio de Janeiro, Rio de Janeiro, Brazil

W.L. Aldá Júnior, E. Belchior Batista Das Chagas, H. BRANDAO MALBOUISSON, W. Carvalho, J. Chinellato⁵, E. Coelho, E.M. Da Costa, G.G. Da Silveira⁶, D. De Jesus Damiao, S. Fonseca De Souza, J. Martins⁷, D. Matos Figueiredo, M. Medina Jaime⁸, M. Melo De Almeida, C. Mora Herrera, L. Mundim, H. Nogima, P. Rebello Teles, L.J. Sanchez Rosas, A. Santoro, S.M. Silva Do Amaral, A. Sznajder, M. Thiel, E.J. Tonelli Manganote⁵, F. Torres Da Silva De Araujo, A. Vilela Pereira

Universidade Estadual Paulista ^a, Universidade Federal do ABC ^b, São Paulo, Brazil

C.A. Bernardes^a, L. Calligaris^a, T.R. Fernandez Perez Tomei^a, E.M. Gregores^b, D.S. Lemos^a, P.G. Mercadante^b, S.F. Novaes^a, Sandra S. Padula^a

Institute for Nuclear Research and Nuclear Energy, Bulgarian Academy of Sciences, Sofia, Bulgaria

A. Aleksandrov, G. Antchev, I. Atanasov, R. Hadjiiska, P. Iaydjiev, M. Misheva, M. Rodozov, M. Shopova, G. Sultanov

University of Sofia, Sofia, Bulgaria

M. Bonchev, A. Dimitrov, T. Ivanov, L. Litov, B. Pavlov, P. Petkov, A. Petrov

Beihang University, Beijing, China

W. Fang³, Q. Guo, H. Wang, L. Yuan

Department of Physics, Tsinghua University, Beijing, China

M. Ahmad, Z. Hu, Y. Wang

Institute of High Energy Physics, Beijing, China

E. Chapon, G.M. Chen⁹, H.S. Chen⁹, M. Chen, A. Kapoor, D. Leggat, H. Liao, Z. Liu, R. Sharma, A. Spiezia, J. Tao, J. Thomas-wilsker, J. Wang, H. Zhang, S. Zhang⁹, J. Zhao

State Key Laboratory of Nuclear Physics and Technology, Peking University, Beijing, China

A. Agapitos, Y. Ban, C. Chen, Q. Huang, A. Levin, Q. Li, M. Lu, X. Lyu, Y. Mao, S.J. Qian, D. Wang, Q. Wang, J. Xiao

Sun Yat-Sen University, Guangzhou, China

Z. You

Institute of Modern Physics and Key Laboratory of Nuclear Physics and Ion-beam Application (MOE) - Fudan University, Shanghai, China

X. Gao³

Zhejiang University, Hangzhou, China

M. Xiao

Universidad de Los Andes, Bogota, Colombia

C. Avila, A. Cabrera, C. Florez, J. Fraga, A. Sarkar, M.A. Segura Delgado

Universidad de Antioquia, Medellin, Colombia

J. Jaramillo, J. Mejia Guisao, F. Ramirez, J.D. Ruiz Alvarez, C.A. Salazar González, N. Vanegas Arbelaez

University of Split, Faculty of Electrical Engineering, Mechanical Engineering and Naval Architecture, Split, Croatia

D. Giljanovic, N. Godinovic, D. Lelas, I. Puljak, T. Sculac

University of Split, Faculty of Science, Split, Croatia

Z. Antunovic, M. Kovac

Institute Rudjer Boskovic, Zagreb, Croatia

V. Brigljevic, D. Ferencek, D. Majumder, M. Roguljic, A. Starodumov¹⁰, T. Susa

University of Cyprus, Nicosia, Cyprus

M.W. Ather, A. Attikis, E. Erodotou, A. Ioannou, G. Kole, M. Kolosova, S. Konstantinou, G. Mavromanolakis, J. Mousa, C. Nicolaou, F. Ptochos, P.A. Razis, H. Rykaczewski, H. Saka, D. Tsiakkouri

Charles University, Prague, Czech Republic

M. Finger¹¹, M. Finger Jr.¹¹, A. Kveton, J. Tomsa

Escuela Politecnica Nacional, Quito, Ecuador

E. Ayala

Universidad San Francisco de Quito, Quito, Ecuador

E. Carrera Jarrin

Academy of Scientific Research and Technology of the Arab Republic of Egypt, Egyptian Network of High Energy Physics, Cairo, Egypt

A.A. Abdelalim^{12,13}, S. Elgammal¹⁴, A. Ellithi Kamel¹⁵

Center for High Energy Physics (CHEP-FU), Fayoum University, El-Fayoum, Egypt

A. Lotfy, M.A. Mahmoud

National Institute of Chemical Physics and Biophysics, Tallinn, Estonia

S. Bhowmik, A. Carvalho Antunes De Oliveira, R.K. Dewanjee, K. Ehataht, M. Kadastik, M. Raidal, C. Veelken

Department of Physics, University of Helsinki, Helsinki, Finland

P. Eerola, L. Forthomme, H. Kirschenmann, K. Osterberg, M. Voutilainen

Helsinki Institute of Physics, Helsinki, Finland

E. Brücken, F. Garcia, J. Havukainen, V. Karimäki, M.S. Kim, R. Kinnunen, T. Lampén, K. Lassila-Perini, S. Laurila, S. Lehti, T. Lindén, H. Siikonen, E. Tuominen, J. Tuominiemi

Lappeenranta University of Technology, Lappeenranta, Finland

P. Luukka, T. Tuuva

IRFU, CEA, Université Paris-Saclay, Gif-sur-Yvette, France

C. Amendola, M. Besancon, F. Couderc, M. Dejardin, D. Denegri, J.L. Faure, F. Ferri, S. Ganjour, A. Givernaud, P. Gras, G. Hamel de Monchenault, P. Jarry, B. Lenzi, E. Locci, J. Malcles, J. Rander, A. Rosowsky, M.Ö. Sahin, A. Savoy-Navarro¹⁶, M. Titov, G.B. Yu

Laboratoire Leprince-Ringuet, CNRS/IN2P3, Ecole Polytechnique, Institut Polytechnique de Paris, Paris, France

S. Ahuja, F. Beaudette, M. Bonanomi, A. Buchot Perraguin, P. Busson, C. Charlot, O. Davignon, B. Diab, G. Falmagne, R. Granier de Cassagnac, A. Hakimi, I. Kucher, A. Lobanov, C. Martin Perez, M. Nguyen, C. Ochando, P. Paganini, J. Rembser, R. Salerno, J.B. Sauvan, Y. Sirois, A. Zabi, A. Zghiche

Université de Strasbourg, CNRS, IPHC UMR 7178, Strasbourg, France

J.-L. Agram¹⁷, J. Andrea, D. Bloch, G. Bourgatte, J.-M. Brom, E.C. Chabert, C. Collard, J.-C. Fontaine¹⁷, D. Gelé, U. Goerlach, C. Grimault, A.-C. Le Bihan, P. Van Hove

Université de Lyon, Université Claude Bernard Lyon 1, CNRS-IN2P3, Institut de Physique Nucléaire de Lyon, Villeurbanne, France

E. Asilar, S. Beauceron, C. Bernet, G. Boudoul, C. Camen, A. Carle, N. Chanon, D. Contardo, P. Depasse, H. El Mamouni, J. Fay, S. Gascon, M. Gouzevitch, B. Ille, Sa. Jain, I.B. Laktineh, H. Lattaud, A. Lesauvage, M. Lethuillier, L. Mirabito, L. Torterotot, G. Touquet, M. Vander Donckt, S. Viret

Georgian Technical University, Tbilisi, Georgia

I. Bagaturia¹⁸, Z. Tsamalaidze¹¹

RWTH Aachen University, I. Physikalisches Institut, Aachen, Germany

L. Feld, K. Klein, M. Lipinski, D. Meuser, A. Pauls, M. Preuten, M.P. Rauch, J. Schulz, M. Teroerde

RWTH Aachen University, III. Physikalisches Institut A, Aachen, Germany

D. Eliseev, M. Erdmann, P. Fackeldey, B. Fischer, S. Ghosh, T. Hebbeker, K. Hoepfner, H. Keller, L. Mastrolorenzo, M. Merschmeyer, A. Meyer, P. Millet, G. Mocellin, S. Mondal, S. Mukherjee,

D. Noll, A. Novak, T. Pook, A. Pozdnyakov, T. Quast, M. Radziej, Y. Rath, H. Reithler, J. Roemer, A. Schmidt, S.C. Schuler, A. Sharma, S. Wiedenbeck, S. Zaleski

RWTH Aachen University, III. Physikalisches Institut B, Aachen, Germany

C. Dziwok, G. Flügge, W. Haj Ahmad¹⁹, O. Hlushchenko, T. Kress, A. Nowack, C. Pistone, O. Pooth, D. Roy, H. Sert, A. Stahl²⁰, T. Ziemons

Deutsches Elektronen-Synchrotron, Hamburg, Germany

H. Aarup Petersen, M. Aldaya Martin, P. Asmuss, I. Babounikau, S. Baxter, O. Behnke, A. Bermúdez Martínez, A.A. Bin Anuar, K. Borrás²¹, V. Botta, D. Brunner, A. Campbell, A. Cardini, P. Connor, S. Consuegra Rodríguez, V. Danilov, A. De Wit, M.M. Defranchis, L. Didukh, D. Domínguez Damiani, G. Eckerlin, D. Eckstein, T. Eichhorn, L.I. Estevez Banos, E. Gallo²², A. Geiser, A. Giraldi, A. Grohsjean, M. Guthoff, A. Harb, A. Jafari²³, N.Z. Jomhari, H. Jung, A. Kasem²¹, M. Kasemann, H. Kaveh, C. Kleinwort, J. Knolle, D. Krücker, W. Lange, T. Lenz, J. Lidrych, K. Lipka, W. Lohmann²⁴, R. Mankel, I.-A. Melzer-Pellmann, J. Metwally, A.B. Meyer, M. Meyer, M. Missiroli, J. Mnich, A. Mussgiller, V. Myronenko, Y. Otari, D. Pérez Adán, S.K. Pflitsch, D. Pitzl, A. Raspereza, A. Saggio, A. Saibel, M. Savitskyi, V. Scheurer, P. Schütze, C. Schwanenberger, A. Singh, R.E. Sosa Ricardo, N. Tonon, O. Turkot, A. Vagnerini, M. Van De Klundert, R. Walsh, D. Walter, Y. Wen, K. Wichmann, C. Wissing, S. Wuchterl, O. Zenaiev, R. Zlebick

University of Hamburg, Hamburg, Germany

R. Aggleton, S. Bein, L. Benato, A. Benecke, K. De Leo, T. Dreyer, A. Ebrahimi, M. Eich, F. Feindt, A. Fröhlich, C. Garbers, E. Garutti, P. Gunnellini, J. Haller, A. Hinzmann, A. Karavdina, G. Kasieczka, R. Klanner, R. Kogler, V. Kutzner, J. Lange, T. Lange, A. Malara, C.E.N. Niemeyer, A. Nigamova, K.J. Pena Rodriguez, O. Rieger, P. Schleper, S. Schumann, J. Schwandt, D. Schwarz, J. Sonneveld, H. Stadie, G. Steinbrück, B. Vormwald, I. Zoi

Karlsruher Institut fuer Technologie, Karlsruhe, Germany

M. Baselga, S. Baur, J. Bechtel, T. Berger, E. Butz, R. Caspart, T. Chwalek, W. De Boer, A. Dierlamm, A. Droll, K. El Morabit, N. Faltermann, K. Flöh, M. Giffels, A. Gottmann, F. Hartmann²⁰, C. Heidecker, U. Husemann, M.A. Iqbal, I. Katkov²⁵, P. Keicher, R. Koppenhöfer, S. Maier, M. Metzler, S. Mitra, D. Müller, Th. Müller, M. Musich, G. Quast, K. Rabbertz, J. Rauser, D. Savoii, D. Schäfer, M. Schnepf, M. Schröder, D. Seith, I. Shvetsov, H.J. Simonis, R. Ulrich, M. Wassmer, M. Weber, R. Wolf, S. Wozniowski

Institute of Nuclear and Particle Physics (INPP), NCSR Demokritos, Aghia Paraskevi, Greece

G. Anagnostou, P. Asenov, G. Daskalakis, T. Gerasis, A. Kyriakis, D. Loukas, G. Paspalaki, A. Stakia

National and Kapodistrian University of Athens, Athens, Greece

M. Diamantopoulou, D. Karasavvas, G. Karathanasis, P. Kontaxakis, C.K. Koraka, A. Manousakis-katsikakis, A. Panagiotou, I. Papavergou, N. Saoulidou, K. Theofilatos, K. Vellidis, E. Vourliotis

National Technical University of Athens, Athens, Greece

G. Bakas, K. Kousouris, I. Papakrivopoulos, G. Tsipolitis, A. Zacharopoulou

University of Ioánnina, Ioánnina, Greece

I. Evangelou, C. Foudas, P. Giannelis, P. Katsoulis, P. Kokkas, S. Mallios, K. Manitaras, N. Manthos, I. Papadopoulos, J. Strolagos

MTA-ELTE Lendület CMS Particle and Nuclear Physics Group, Eötvös Loránd University, Budapest, Hungary

M. Bartók²⁶, R. Chudasama, M. Csanad, M.M.A. Gadallah²⁷, S. Lökös²⁸, P. Major, K. Mandal, A. Mehta, G. Pasztor, O. Surányi, G.I. Veres

Wigner Research Centre for Physics, Budapest, Hungary

G. Bencze, C. Hajdu, D. Horvath²⁹, F. Sikler, V. Veszpremi, G. Vesztergombi[†]

Institute of Nuclear Research ATOMKI, Debrecen, Hungary

S. Czellar, J. Karancsi²⁶, J. Molnar, Z. Szillasi, D. Teyssier

Institute of Physics, University of Debrecen, Debrecen, Hungary

P. Raics, Z.L. Trocsanyi, B. Ujvari

Eszterhazy Karoly University, Karoly Robert Campus, Gyongyos, Hungary

T. Csorgo, F. Nemes, T. Novak

Indian Institute of Science (IISc), Bangalore, India

S. Choudhury, J.R. Komaragiri, D. Kumar, L. Panwar, P.C. Tiwari

National Institute of Science Education and Research, HBNI, Bhubaneswar, India

S. Bahinipati³⁰, D. Dash, C. Kar, P. Mal, T. Mishra, V.K. Muraleedharan Nair Bindhu, A. Nayak³¹, D.K. Sahoo³⁰, N. Sur, S.K. Swain

Panjab University, Chandigarh, India

S. Bansal, S.B. Beri, V. Bhatnagar, S. Chauhan, N. Dhingra³², R. Gupta, A. Kaur, S. Kaur, P. Kumari, M. Lohan, M. Meena, K. Sandeep, S. Sharma, J.B. Singh, A.K. Viridi

University of Delhi, Delhi, India

A. Ahmed, A. Bhardwaj, B.C. Choudhary, R.B. Garg, M. Gola, S. Keshri, A. Kumar, M. Naimuddin, P. Priyanka, K. Ranjan, A. Shah

Saha Institute of Nuclear Physics, HBNI, Kolkata, India

M. Bharti³³, R. Bhattacharya, S. Bhattacharya, D. Bhowmik, S. Dutta, S. Ghosh, B. Gomber³⁴, M. Maity³⁵, S. Nandan, P. Palit, A. Purohit, P.K. Rout, G. Saha, S. Sarkar, M. Sharan, B. Singh³³, S. Thakur³³

Indian Institute of Technology Madras, Madras, India

P.K. Behera, S.C. Behera, P. Kalbhor, A. Muhammad, R. Pradhan, P.R. Pujahari, A. Sharma, A.K. Sikdar

Bhabha Atomic Research Centre, Mumbai, India

D. Dutta, V. Kumar, K. Naskar³⁶, P.K. Netrakanti, L.M. Pant, P. Shukla

Tata Institute of Fundamental Research-A, Mumbai, India

T. Aziz, M.A. Bhat, S. Dugad, R. Kumar Verma, G.B. Mohanty, U. Sarkar

Tata Institute of Fundamental Research-B, Mumbai, India

S. Banerjee, S. Bhattacharya, S. Chatterjee, M. Guchait, S. Karmakar, S. Kumar, G. Majumder, K. Mazumdar, S. Mukherjee, D. Roy, N. Sahoo

Indian Institute of Science Education and Research (IISER), Pune, India

S. Dube, B. Kansal, K. Kothekar, S. Pandey, A. Rane, A. Rastogi, S. Sharma

Department of Physics, Isfahan University of Technology, Isfahan, Iran

H. Bakhshiansohi³⁷

Institute for Research in Fundamental Sciences (IPM), Tehran, Iran

S. Chenarani³⁸, S.M. Etesami, M. Khakzad, M. Mohammadi Najafabadi

University College Dublin, Dublin, Ireland

M. Felcini, M. Grunewald

INFN Sezione di Bari ^a, Università di Bari ^b, Politecnico di Bari ^c, Bari, Italy

M. Abbrescia^{a,b}, R. Aly^{a,b,39}, C. Aruta^{a,b}, A. Colaleo^a, D. Creanza^{a,c}, N. De Filippis^{a,c}, M. De Palma^{a,b}, A. Di Florio^{a,b}, A. Di Pilato^{a,b}, W. Elmetenawee^{a,b}, L. Fiore^a, A. Gelmi^{a,b}, M. Gul^a, G. Iaselli^{a,c}, M. Ince^{a,b}, S. Lezki^{a,b}, G. Maggi^{a,c}, M. Maggi^a, I. Margjeka^{a,b}, V. Mastrapasqua^{a,b}, J.A. Merlin^a, S. My^{a,b}, S. Nuzzo^{a,b}, A. Pompili^{a,b}, G. Pugliese^{a,c}, A. Ranieri^a, G. Selvaggi^{a,b}, L. Silvestris^a, F.M. Simone^{a,b}, R. Venditti^a, P. Verwilligen^a

INFN Sezione di Bologna ^a, Università di Bologna ^b, Bologna, Italy

G. Abbiendi^a, C. Battilana^{a,b}, D. Bonacorsi^{a,b}, L. Borgonovi^{a,b}, S. Braibant-Giacomelli^{a,b}, R. Campanini^{a,b}, P. Capiluppi^{a,b}, A. Castro^{a,b}, F.R. Cavallo^a, M. Cuffiani^{a,b}, G.M. Dallavalle^a, T. Diotallevi^{a,b}, F. Fabbri^a, A. Fanfani^{a,b}, E. Fontanesi^{a,b}, P. Giacomelli^a, L. Giommi^{a,b}, C. Grandi^a, L. Guiducci^{a,b}, F. Iemmi^{a,b}, S. Lo Meo^{a,40}, S. Marcellini^a, G. Masetti^a, F.L. Navarria^{a,b}, A. Perrotta^a, F. Primavera^{a,b}, A.M. Rossi^{a,b}, T. Rovelli^{a,b}, G.P. Siroli^{a,b}, N. Tosi^a

INFN Sezione di Catania ^a, Università di Catania ^b, Catania, Italy

S. Albergo^{a,b,41}, S. Costa^{a,b}, A. Di Mattia^a, R. Potenza^{a,b}, A. Tricomi^{a,b,41}, C. Tuve^{a,b}

INFN Sezione di Firenze ^a, Università di Firenze ^b, Firenze, Italy

G. Barbaglia^a, A. Cassese^a, R. Ceccarelli^{a,b}, V. Ciulli^{a,b}, C. Civinini^a, R. D'Alessandro^{a,b}, F. Fiori^a, E. Focardi^{a,b}, G. Latino^{a,b}, P. Lenzi^{a,b}, M. Lizzo^{a,b}, M. Meschini^a, S. Paoletti^a, R. Seidita^{a,b}, G. Sguazzoni^a, L. Viliani^a

INFN Laboratori Nazionali di Frascati, Frascati, Italy

L. Benussi, S. Bianco, D. Piccolo

INFN Sezione di Genova ^a, Università di Genova ^b, Genova, Italy

M. Bozzo^{a,b}, F. Ferro^a, R. Mulargia^{a,b}, E. Robutti^a, S. Tosi^{a,b}

INFN Sezione di Milano-Bicocca ^a, Università di Milano-Bicocca ^b, Milano, Italy

A. Benaglia^a, A. Beschi^{a,b}, F. Brivio^{a,b}, F. Ceteorelli^{a,b}, V. Ciriolo^{a,b,20}, F. De Guio^{a,b}, M.E. Dinardo^{a,b}, P. Dini^a, S. Gennai^a, A. Ghezzi^{a,b}, P. Govoni^{a,b}, L. Guzzi^{a,b}, M. Malberti^a, S. Malvezzi^a, D. Menasce^a, F. Monti^{a,b}, L. Moroni^a, M. Paganoni^{a,b}, D. Pedrini^a, S. Ragazzi^{a,b}, T. Tabarelli de Fatis^{a,b}, D. Valsecchi^{a,b,20}, D. Zuolo^{a,b}

INFN Sezione di Napoli ^a, Università di Napoli 'Federico II' ^b, Napoli, Italy, Università della Basilicata ^c, Potenza, Italy, Università G. Marconi ^d, Roma, Italy

S. Buontempo^a, N. Cavallo^{a,c}, A. De Iorio^{a,b}, F. Fabozzi^{a,c}, F. Fienga^a, A.O.M. Iorio^{a,b}, L. Lista^{a,b}, S. Meola^{a,d,20}, P. Paolucci^{a,20}, B. Rossi^a, C. Sciacca^{a,b}, E. Voevodina^{a,b}

INFN Sezione di Padova ^a, Università di Padova ^b, Padova, Italy, Università di Trento ^c, Trento, Italy

P. Azzi^a, N. Bacchetta^a, D. Bisello^{a,b}, A. Boletti^{a,b}, A. Bragagnolo^{a,b}, R. Carlin^{a,b}, P. Checchia^a, P. De Castro Manzano^a, T. Dorigo^a, F. Gasparini^{a,b}, U. Gasparini^{a,b}, S.Y. Hoh^{a,b}, L. Layer^{a,42}, M. Margoni^{a,b}, A.T. Meneguzzo^{a,b}, M. Presilla^b, P. Ronchese^{a,b}, R. Rossin^{a,b}, F. Simonetto^{a,b}, G. Strong, A. Tiko^a, M. Tosi^{a,b}, H. YARAR^{a,b}, M. Zanetti^{a,b}, P. Zotto^{a,b}, A. Zucchetta^{a,b}, G. Zumerle^{a,b}

INFN Sezione di Pavia ^a, Università di Pavia ^b, Pavia, Italy

C. Aime^{a,b}, A. Braghieri^a, S. Calzaferri^{a,b}, D. Fiorina^{a,b}, P. Montagna^{a,b}, S.P. Ratti^{a,b}, V. Re^a, M. Ressegotti^{a,b}, C. Riccardi^{a,b}, P. Salvini^a, I. Vai^a, P. Vitulo^{a,b}

INFN Sezione di Perugia ^a, Università di Perugia ^b, Perugia, Italy

M. Biasini^{a,b}, G.M. Bilei^a, D. Ciangottini^{a,b}, L. Fanò^{a,b}, P. Lariccia^{a,b}, G. Mantovani^{a,b}, V. Mariani^{a,b}, M. Menichelli^a, F. Moscatelli^a, A. Piccinelli^{a,b}, A. Rossi^{a,b}, A. Santocchia^{a,b}, D. Spiga^a, T. Tedeschi^{a,b}

INFN Sezione di Pisa ^a, Università di Pisa ^b, Scuola Normale Superiore di Pisa ^c, Pisa, Italy

K. Androsov^a, P. Azzurri^a, G. Bagliesi^a, V. Bertacchi^{a,c}, L. Bianchini^a, T. Boccali^a, R. Castaldi^a, M.A. Ciocci^{a,b}, R. Dell'Orso^a, M.R. Di Domenico^{a,b}, S. Donato^a, L. Giannini^{a,c}, A. Giassi^a, M.T. Grippo^a, F. Ligabue^{a,c}, E. Manca^{a,c}, G. Mandorli^{a,c}, A. Messineo^{a,b}, F. Palla^a, G. Ramirez-Sanchez^{a,c}, A. Rizzi^{a,b}, G. Rolandi^{a,c}, S. Roy Chowdhury^{a,c}, A. Scribano^a, N. Shafiei^{a,b}, P. Spagnolo^a, R. Tenchini^a, G. Tonelli^{a,b}, N. Turini^a, A. Venturi^a, P.G. Verdini^a

INFN Sezione di Roma ^a, Sapienza Università di Roma ^b, Rome, Italy

F. Cavallari^a, M. Cipriani^{a,b}, D. Del Re^{a,b}, E. Di Marco^a, M. Diemoz^a, E. Longo^{a,b}, P. Meridiani^a, G. Organtini^{a,b}, F. Pandolfi^a, R. Paramatti^{a,b}, C. Quaranta^{a,b}, S. Rahatlou^{a,b}, C. Rovelli^a, F. Santanastasio^{a,b}, L. Soffi^{a,b}, R. Tramontano^{a,b}

INFN Sezione di Torino ^a, Università di Torino ^b, Torino, Italy, Università del Piemonte Orientale ^c, Novara, Italy

N. Amapane^{a,b}, R. Arcidiacono^{a,c}, S. Argiro^{a,b}, M. Arneodo^{a,c}, N. Bartosik^a, R. Bellan^{a,b}, A. Bellora^{a,b}, C. Biino^a, A. Cappati^{a,b}, N. Cartiglia^a, S. Cometti^a, M. Costa^{a,b}, R. Covarelli^{a,b}, N. Demaria^a, B. Kiani^{a,b}, F. Legger^a, C. Mariotti^a, S. Maselli^a, E. Migliore^{a,b}, V. Monaco^{a,b}, E. Monteil^{a,b}, M. Monteno^a, M.M. Obertino^{a,b}, G. Ortona^a, L. Pacher^{a,b}, N. Pastrone^a, M. Pelliccioni^a, G.L. Pinna Angioni^{a,b}, M. Ruspa^{a,c}, R. Salvatico^{a,b}, F. Siviero^{a,b}, V. Sola^a, A. Solano^{a,b}, D. Soldi^{a,b}, A. Staiano^a, D. Trocino^{a,b}

INFN Sezione di Trieste ^a, Università di Trieste ^b, Trieste, Italy

S. Belforte^a, V. Candelise^{a,b}, M. Casarsa^a, F. Cossutti^a, A. Da Rold^{a,b}, G. Della Ricca^{a,b}, F. Vazzoler^{a,b}

Kyungpook National University, Daegu, Korea

S. Dogra, C. Huh, B. Kim, D.H. Kim, G.N. Kim, J. Lee, S.W. Lee, C.S. Moon, Y.D. Oh, S.I. Pak, B.C. Radburn-Smith, S. Sekmen, Y.C. Yang

Chonnam National University, Institute for Universe and Elementary Particles, Kwangju, Korea

H. Kim, D.H. Moon

Hanyang University, Seoul, Korea

B. Francois, T.J. Kim, J. Park

Korea University, Seoul, Korea

S. Cho, S. Choi, Y. Go, S. Ha, B. Hong, K. Lee, K.S. Lee, J. Lim, J. Park, S.K. Park, J. Yoo

Kyung Hee University, Department of Physics, Seoul, Republic of Korea

J. Goh, A. Gurtu

Sejong University, Seoul, Korea

H.S. Kim, Y. Kim

Seoul National University, Seoul, Korea

J. Almond, J.H. Bhyun, J. Choi, S. Jeon, J. Kim, J.S. Kim, S. Ko, H. Kwon, H. Lee, K. Lee, S. Lee, K. Nam, B.H. Oh, M. Oh, S.B. Oh, H. Seo, U.K. Yang, I. Yoon

University of Seoul, Seoul, Korea

D. Jeon, J.H. Kim, B. Ko, J.S.H. Lee, I.C. Park, Y. Roh, D. Song, I.J. Watson

Yonsei University, Department of Physics, Seoul, Korea

H.D. Yoo

Sungkyunkwan University, Suwon, Korea

Y. Choi, C. Hwang, Y. Jeong, H. Lee, Y. Lee, I. Yu

Riga Technical University, Riga, Latvia

V. Veckalns⁴³

Vilnius University, Vilnius, Lithuania

A. Juodagalvis, A. Rinkevicius, G. Tamulaitis

National Centre for Particle Physics, Universiti Malaya, Kuala Lumpur, Malaysia

W.A.T. Wan Abdullah, M.N. Yusli, Z. Zolkapli

Universidad de Sonora (UNISON), Hermosillo, Mexico

J.F. Benitez, A. Castaneda Hernandez, J.A. Murillo Quijada, L. Valencia Palomo

Centro de Investigacion y de Estudios Avanzados del IPN, Mexico City, Mexico

H. Castilla-Valdez, E. De La Cruz-Burelo, I. Heredia-De La Cruz⁴⁴, R. Lopez-Fernandez, A. Sanchez-Hernandez

Universidad Iberoamericana, Mexico City, Mexico

S. Carrillo Moreno, C. Oropeza Barrera, M. Ramirez-Garcia, F. Vazquez Valencia

Benemerita Universidad Autonoma de Puebla, Puebla, Mexico

J. Eysermans, I. Pedraza, H.A. Salazar Ibarquen, C. Uribe Estrada

Universidad Autónoma de San Luis Potosí, San Luis Potosí, Mexico

A. Morelos Pineda

University of Montenegro, Podgorica, Montenegro

J. Mijuskovic⁴, N. Raicevic

University of Auckland, Auckland, New Zealand

D. Krofcheck

University of Canterbury, Christchurch, New Zealand

S. Bheesette, P.H. Butler

National Centre for Physics, Quaid-I-Azam University, Islamabad, Pakistan

A. Ahmad, M.I. Asghar, M.I.M. Awan, H.R. Hoorani, W.A. Khan, M.A. Shah, M. Shoaib, M. Waqas

AGH University of Science and Technology Faculty of Computer Science, Electronics and Telecommunications, Krakow, Poland

V. Avati, L. Grzanka, M. Malawski

National Centre for Nuclear Research, Swierk, Poland

H. Bialkowska, M. Bluj, B. Boimska, T. Frueboes, M. Górski, M. Kazana, M. Szleper, P. Traczyk, P. Zalewski

Institute of Experimental Physics, Faculty of Physics, University of Warsaw, Warsaw, Poland
K. Bunkowski, A. Byszuk⁴⁵, K. Doroba, A. Kalinowski, M. Konecki, J. Krolikowski,
M. Olszewski, M. Walczak

Laboratório de Instrumentação e Física Experimental de Partículas, Lisboa, Portugal
M. Araujo, P. Bargassa, D. Bastos, P. Faccioli, M. Gallinaro, J. Hollar, N. Leonardo, T. Niknejad,
J. Seixas, K. Shchelina, O. Toldaiev, J. Varela

Joint Institute for Nuclear Research, Dubna, Russia
S. Afanasiev, P. Bunin, M. Gavrilenko, I. Golutvin, I. Gorbunov, A. Kamenev, V. Karjavine,
A. Lanev, A. Malakhov, V. Matveev^{46,47}, P. Moiseenz, V. Palichik, V. Perelygin, M. Savina,
D. Seitova, V. Shalaev, S. Shmatov, S. Shulha, V. Smirnov, O. Teryaev, N. Voytishin, A. Zarubin,
I. Zhizhin

Petersburg Nuclear Physics Institute, Gatchina (St. Petersburg), Russia
G. Gavrillov, V. Golovtsov, Y. Ivanov, V. Kim⁴⁸, E. Kuznetsova⁴⁹, V. Murzin, V. Oreshkin,
I. Smirnov, D. Sosnov, V. Sulimov, L. Uvarov, S. Volkov, A. Vorobyev

Institute for Nuclear Research, Moscow, Russia
Yu. Andreev, A. Dermenev, S. Gninenko, N. Golubev, A. Karneyeu, M. Kirsanov, N. Krasnikov,
A. Pashenkov, G. Pivovarov, D. Tlisov[†], A. Toropin

**Institute for Theoretical and Experimental Physics named by A.I. Alikhanov of NRC
'Kurchatov Institute', Moscow, Russia**
V. Epshteyn, V. Gavrillov, N. Lychkovskaya, A. Nikitenko⁵⁰, V. Popov, G. Safronov,
A. Spiridonov, A. Stepenov, M. Toms, E. Vlasov, A. Zhokin

Moscow Institute of Physics and Technology, Moscow, Russia
T. Aushev

**National Research Nuclear University 'Moscow Engineering Physics Institute' (MEPhI),
Moscow, Russia**
R. Chistov⁵¹, M. Danilov⁵², A. Oskin, P. Parygin, S. Polikarpov⁵¹

P.N. Lebedev Physical Institute, Moscow, Russia
V. Andreev, M. Azarkin, I. Dremin, M. Kirakosyan, A. Terkulov

**Skobeltsyn Institute of Nuclear Physics, Lomonosov Moscow State University, Moscow,
Russia**
A. Belyaev, E. Boos, V. Bunichev, M. Dubinin⁵³, L. Dudko, A. Ershov, A. Gribushin, V. Klyukhin,
O. Kodolova, I. Lokhtin, S. Obraztsov, V. Savrin, A. Snigirev

Novosibirsk State University (NSU), Novosibirsk, Russia
V. Blinov⁵⁴, T. Dimova⁵⁴, L. Kardapoltsev⁵⁴, I. Ovtin⁵⁴, Y. Skovpen⁵⁴

**Institute for High Energy Physics of National Research Centre 'Kurchatov Institute',
Protvino, Russia**
I. Azhgirey, I. Bayshev, V. Kachanov, A. Kalinin, D. Konstantinov, V. Petrov, R. Ryutin, A. Sobol,
S. Troshin, N. Tyurin, A. Uzunian, A. Volkov

National Research Tomsk Polytechnic University, Tomsk, Russia
A. Babaev, A. Iuzhakov, V. Okhotnikov, L. Sukhikh

Tomsk State University, Tomsk, Russia
V. Borchsh, V. Ivanchenko, E. Tcherniaev

University of Belgrade: Faculty of Physics and VINCA Institute of Nuclear Sciences, Belgrade, Serbia

P. Adzic⁵⁵, P. Cirkovic, M. Dordevic, P. Milenovic, J. Milosevic

Centro de Investigaciones Energéticas Medioambientales y Tecnológicas (CIEMAT), Madrid, Spain

M. Aguilar-Benitez, J. Alcaraz Maestre, A. Álvarez Fernández, I. Bachiller, M. Barrio Luna, Cristina F. Bedoya, J.A. Brochero Cifuentes, C.A. Carrillo Montoya, M. Cepeda, M. Cerrada, N. Colino, B. De La Cruz, A. Delgado Peris, J.P. Fernández Ramos, J. Flix, M.C. Fouz, A. García Alonso, O. Gonzalez Lopez, S. Goy Lopez, J.M. Hernandez, M.I. Josa, J. León Holgado, D. Moran, Á. Navarro Tobar, A. Pérez-Calero Yzquierdo, J. Puerta Pelayo, I. Redondo, L. Romero, S. Sánchez Navas, M.S. Soares, A. Triossi, L. Urda Gómez, C. Willmott

Universidad Autónoma de Madrid, Madrid, Spain

C. Albajar, J.F. de Trocóniz, R. Reyes-Almanza

Universidad de Oviedo, Instituto Universitario de Ciencias y Tecnologías Espaciales de Asturias (ICTEA), Oviedo, Spain

B. Alvarez Gonzalez, J. Cuevas, C. Erice, J. Fernandez Menendez, S. Folgueras, I. Gonzalez Caballero, E. Palencia Cortezon, C. Ramón Álvarez, J. Ripoll Sau, V. Rodríguez Bouza, S. Sanchez Cruz, A. Trapote

Instituto de Física de Cantabria (IFCA), CSIC-Universidad de Cantabria, Santander, Spain

I.J. Cabrillo, A. Calderon, B. Chazin Quero, J. Duarte Campderros, M. Fernandez, P.J. Fernández Manteca, G. Gomez, C. Martinez Rivero, P. Martinez Ruiz del Arbol, F. Matorras, J. Piedra Gomez, C. Prieels, F. Ricci-Tam, T. Rodrigo, A. Ruiz-Jimeno, L. Scodellaro, I. Vila, J.M. Vizan Garcia

University of Colombo, Colombo, Sri Lanka

MK Jayananda, B. Kailasapathy⁵⁶, D.U.J. Sonnadara, DDC Wickramarathna

University of Ruhuna, Department of Physics, Matara, Sri Lanka

W.G.D. Dharmaratna, K. Liyanage, N. Perera, N. Wickramage

CERN, European Organization for Nuclear Research, Geneva, Switzerland

T.K. Aarrestad, D. Abbaneo, B. Akgun, E. Auffray, G. Auzinger, J. Baechler, P. Baillon, A.H. Ball, D. Barney, J. Bendavid, N. Beni, M. Bianco, A. Bocci, P. Bortignon, E. Bossini, E. Brondolin, T. Camporesi, G. Cerminara, L. Cristella, D. d'Enterria, A. Dabrowski, N. Daci, V. Daponte, A. David, A. De Roeck, M. Deile, R. Di Maria, M. Dobson, M. Dünser, N. Dupont, A. Elliott-Peisert, N. Emriskova, F. Fallavollita⁵⁷, D. Fasanella, S. Fiorendi, G. Franzoni, J. Fulcher, W. Funk, S. Giani, D. Gigi, K. Gill, F. Glege, L. Gouskos, M. Guilbaud, D. Gulhan, M. Haranko, J. Hegeman, Y. Iiyama, V. Innocente, T. James, P. Janot, J. Kaspar, J. Kieseler, M. Komm, N. Kratochwil, C. Lange, P. Lecoq, K. Long, C. Lourenço, L. Malgeri, M. Mannelli, A. Massironi, F. Meijers, S. Mersi, E. Meschi, F. Moortgat, M. Mulders, J. Ngadiuba, J. Niedziela, S. Orfanelli, L. Orsini, F. Pantaleo²⁰, L. Pape, E. Perez, M. Peruzzi, A. Petrilli, G. Petrucciani, A. Pfeiffer, M. Pierini, D. Rabad, A. Racz, M. Rieger, M. Rovere, H. Sakulin, J. Salfeld-Nebgen, S. Scarfi, C. Schäfer, C. Schwick, M. Selvaggi, A. Sharma, P. Silva, W. Snoeys, P. Sphicas⁵⁸, J. Steggemann, S. Summers, V.R. Tavolaro, D. Treille, A. Tsirou, G.P. Van Onsem, A. Vartak, M. Verzetti, K.A. Wozniak, W.D. Zeuner

Paul Scherrer Institut, Villigen, Switzerland

L. Caminada⁵⁹, W. Erdmann, R. Horisberger, Q. Ingram, H.C. Kaestli, D. Kotlinski, U. Langenegger, T. Rohe

ETH Zurich - Institute for Particle Physics and Astrophysics (IPA), Zurich, Switzerland

M. Backhaus, P. Berger, A. Calandri, N. Chernyavskaya, A. De Cosa, G. Dissertori, M. Dittmar, M. Donegà, C. Dorfer, T. Gadek, T.A. Gómez Espinosa, C. Grab, D. Hits, W. Luster, A.-M. Lyon, R.A. Manzoni, M.T. Meinhard, F. Micheli, F. Nessi-Tedaldi, F. Pauss, V. Perovic, G. Perrin, L. Perrozzi, S. Pigazzini, M.G. Ratti, M. Reichmann, C. Reissel, T. Reitenspiess, B. Ristic, D. Ruini, D.A. Sanz Becerra, M. Schönenberger, V. Stampf, M.L. Vesterbacka Olsson, R. Wallny, D.H. Zhu

Universität Zürich, Zurich, Switzerland

C. AMSLER⁶⁰, C. Botta, D. Brzhechko, M.F. Canelli, R. Del Burgo, J.K. Heikkilä, M. Huwiler, A. Jofrehei, B. Kilminster, S. Leontsinis, A. Macchiolo, P. Meiring, V.M. Mikuni, U. Molinatti, I. Neutelings, G. Rauco, A. Reimers, P. Robmann, K. Schweiger, Y. Takahashi, S. Wertz

National Central University, Chung-Li, Taiwan

C. Adloff⁶¹, C.M. Kuo, W. Lin, A. Roy, T. Sarkar³⁵, S.S. Yu

National Taiwan University (NTU), Taipei, Taiwan

L. Ceard, P. Chang, Y. Chao, K.F. Chen, P.H. Chen, W.-S. Hou, Y.y. Li, R.-S. Lu, E. Paganis, A. Psallidas, A. Steen, E. Yazgan

Chulalongkorn University, Faculty of Science, Department of Physics, Bangkok, Thailand

B. Asavapibhop, C. Asawatangtrakuldee, N. Srimanobhas

Çukurova University, Physics Department, Science and Art Faculty, Adana, Turkey

F. Boran, S. Damarcekin⁶², Z.S. Demiroglu, F. Dolek, C. Dozen⁶³, I. Dumanoglu⁶⁴, E. Eskut, G. Gokbulut, Y. Guler, E. Gurpinar Guler⁶⁵, I. Hos⁶⁶, C. Isik, E.E. Kangal⁶⁷, O. Kara, A. Kayis Topaksu, U. Kiminsu, G. Onengut, K. Ozdemir⁶⁸, A. Polatoz, A.E. Simsek, B. Tali⁶⁹, U.G. Tok, S. Turkcapar, I.S. Zorbakir, C. Zorbilmez

Middle East Technical University, Physics Department, Ankara, Turkey

B. Isildak⁷⁰, G. Karapinar⁷¹, K. Ocalan⁷², M. Yalvac⁷³

Bogazici University, Istanbul, Turkey

I.O. Atakisi, E. Gülmez, M. Kaya⁷⁴, O. Kaya⁷⁵, Ö. Özçelik, S. Tekten⁷⁶, E.A. Yetkin⁷⁷

Istanbul Technical University, Istanbul, Turkey

A. Cakir, K. Cankocak⁶⁴, Y. Komurcu, S. Sen⁷⁸

Istanbul University, Istanbul, Turkey

F. Aydogmus Sen, S. Cerci⁶⁹, B. Kaynak, S. Ozkorucuklu, D. Sunar Cerci⁶⁹

Institute for Scintillation Materials of National Academy of Science of Ukraine, Kharkov, Ukraine

B. Grynyov

National Scientific Center, Kharkov Institute of Physics and Technology, Kharkov, Ukraine

L. Levchuk

University of Bristol, Bristol, United Kingdom

E. Bhal, S. Bologna, J.J. Brooke, E. Clement, D. Cussans, H. Flacher, J. Goldstein, G.P. Heath, H.F. Heath, L. Kreczko, B. Krikler, S. Paramesvaran, T. Sakuma, S. Seif El Nasr-Storey, V.J. Smith, J. Taylor, A. Titterton

Rutherford Appleton Laboratory, Didcot, United Kingdom

K.W. Bell, A. Belyaev⁷⁹, C. Brew, R.M. Brown, D.J.A. Cockerill, K.V. Ellis, K. Harder,

S. Harper, J. Linacre, K. Manolopoulos, D.M. Newbold, E. Olaiya, D. Petyt, T. Reis, T. Schuh, C.H. Shepherd-Themistocleous, A. Thea, I.R. Tomalin, T. Williams

Imperial College, London, United Kingdom

R. Bainbridge, P. Bloch, S. Bonomally, J. Borg, S. Breeze, O. Buchmuller, A. Bundock, V. Cepaitis, G.S. Chahal⁸⁰, D. Colling, P. Dauncey, G. Davies, M. Della Negra, G. Fedi, G. Hall, G. Iles, J. Langford, L. Lyons, A.-M. Magnan, S. Malik, A. Martelli, V. Milosevic, J. Nash⁸¹, V. Palladino, M. Pesaresi, D.M. Raymond, A. Richards, A. Rose, E. Scott, C. Seez, A. Shtipliyski, M. Stoye, A. Tapper, K. Uchida, T. Virdee²⁰, N. Wardle, S.N. Webb, D. Winterbottom, A.G. Zecchinelli

Brunel University, Uxbridge, United Kingdom

J.E. Cole, P.R. Hobson, A. Khan, P. Kyberd, C.K. Mackay, I.D. Reid, L. Teodorescu, S. Zahid

Baylor University, Waco, USA

A. Brinkerhoff, K. Call, B. Caraway, J. Dittmann, K. Hatakeyama, A.R. Kanuganti, C. Madrid, B. McMaster, N. Pastika, S. Sawant, C. Smith, J. Wilson

Catholic University of America, Washington, DC, USA

R. Bartek, A. Dominguez, R. Uniyal, A.M. Vargas Hernandez

The University of Alabama, Tuscaloosa, USA

A. Buccilli, O. Charaf, S.I. Cooper, S.V. Gleyzer, C. Henderson, P. Rumerio, C. West

Boston University, Boston, USA

A. Akpinar, A. Albert, D. Arcaro, C. Cosby, Z. Demiragli, D. Gastler, C. Richardson, J. Rohlf, K. Salyer, D. Sperka, D. Spitzbart, I. Suarez, S. Yuan, D. Zou

Brown University, Providence, USA

G. Benelli, B. Burkle, X. Coubez²¹, D. Cutts, Y.t. Duh, M. Hadley, U. Heintz, J.M. Hogan⁸², K.H.M. Kwok, E. Laird, G. Landsberg, K.T. Lau, J. Lee, M. Narain, S. Sagir⁸³, R. Syarif, E. Usai, W.Y. Wong, D. Yu, W. Zhang

University of California, Davis, Davis, USA

R. Band, C. Brainerd, R. Breedon, M. Calderon De La Barca Sanchez, M. Chertok, J. Conway, R. Conway, P.T. Cox, R. Erbacher, C. Flores, G. Funk, F. Jensen, W. Ko[†], O. Kukral, R. Lander, M. Mulhearn, D. Pellett, J. Pilot, M. Shi, D. Taylor, K. Tos, M. Tripathi, Y. Yao, F. Zhang

University of California, Los Angeles, USA

M. Bachtis, R. Cousins, A. Dasgupta, A. Florent, D. Hamilton, J. Hauser, M. Ignatenko, T. Lam, N. Mccoll, W.A. Nash, S. Regnard, D. Saltzberg, C. Schnaible, B. Stone, V. Valuev

University of California, Riverside, Riverside, USA

K. Burt, Y. Chen, R. Clare, J.W. Gary, S.M.A. Ghiasi Shirazi, G. Hanson, G. Karapostoli, O.R. Long, N. Manganeli, M. Olmedo Negrete, M.I. Paneva, W. Si, S. Wimpenny, Y. Zhang

University of California, San Diego, La Jolla, USA

J.G. Branson, P. Chang, S. Cittolin, S. Cooperstein, N. Deelen, M. Derdzinski, J. Duarte, R. Gerosa, D. Gilbert, B. Hashemi, V. Krutelyov, J. Letts, M. Masciovecchio, S. May, S. Padhi, M. Pieri, V. Sharma, M. Tadel, F. Würthwein, A. Yagil

University of California, Santa Barbara - Department of Physics, Santa Barbara, USA

N. Amin, C. Campagnari, M. Citron, A. Dorsett, V. Dutta, J. Incandela, B. Marsh, H. Mei, A. Ovcharova, H. Qu, M. Quinnan, J. Richman, U. Sarica, D. Stuart, S. Wang

California Institute of Technology, Pasadena, USA

D. Anderson, A. Bornheim, O. Cerri, I. Dutta, J.M. Lawhorn, N. Lu, J. Mao, H.B. Newman, T.Q. Nguyen, J. Pata, M. Spiropulu, J.R. Vlimant, S. Xie, Z. Zhang, R.Y. Zhu

Carnegie Mellon University, Pittsburgh, USA

J. Alison, M.B. Andrews, T. Ferguson, T. Mudholkar, M. Paulini, M. Sun, I. Vorobiev

University of Colorado Boulder, Boulder, USA

J.P. Cumalat, W.T. Ford, E. MacDonald, T. Mulholland, R. Patel, A. Perloff, K. Stenson, K.A. Ulmer, S.R. Wagner

Cornell University, Ithaca, USA

J. Alexander, Y. Cheng, J. Chu, D.J. Cranshaw, A. Datta, A. Frankenthal, K. Mcdermott, J. Monroy, J.R. Patterson, D. Quach, A. Ryd, W. Sun, S.M. Tan, Z. Tao, J. Thom, P. Wittich, M. Zientek

Fermi National Accelerator Laboratory, Batavia, USA

S. Abdullin, M. Albrow, M. Alyari, G. Apollinari, A. Apresyan, A. Apyan, S. Banerjee, L.A.T. Bauerdick, A. Beretvas, D. Berry, J. Berryhill, P.C. Bhat, K. Burkett, J.N. Butler, A. Canepa, G.B. Cerati, H.W.K. Cheung, F. Chlebana, M. Cremonesi, V.D. Elvira, J. Freeman, Z. Gecse, E. Gottschalk, L. Gray, D. Green, S. Grünendahl, O. Gutsche, R.M. Harris, S. Hasegawa, R. Heller, T.C. Herwig, J. Hirschauer, B. Jayatilaka, S. Jindariani, M. Johnson, U. Joshi, P. Klabbers, T. Klijnsma, B. Klima, M.J. Kortelainen, S. Lammel, D. Lincoln, R. Lipton, M. Liu, T. Liu, J. Lykken, K. Maeshima, D. Mason, P. McBride, P. Merkel, S. Mrenna, S. Nahn, V. O'Dell, V. Papadimitriou, K. Pedro, C. Pena⁵³, O. Prokofyev, F. Ravera, A. Reinsvold Hall, L. Ristori, B. Schneider, E. Sexton-Kennedy, N. Smith, A. Soha, W.J. Spalding, L. Spiegel, S. Stoynev, J. Strait, L. Taylor, S. Tkaczyk, N.V. Tran, L. Uplegger, E.W. Vaandering, H.A. Weber, A. Woodard

University of Florida, Gainesville, USA

D. Acosta, P. Avery, D. Bourilkov, L. Cadamuro, V. Cherepanov, F. Errico, R.D. Field, D. Guerrero, B.M. Joshi, M. Kim, J. Konigsberg, A. Korytov, K.H. Lo, K. Matchev, N. Menendez, G. Mitselmakher, D. Rosenzweig, K. Shi, J. Wang, S. Wang, X. Zuo

Florida State University, Tallahassee, USA

T. Adams, A. Askew, D. Diaz, R. Habibullah, S. Hagopian, V. Hagopian, K.F. Johnson, R. Khurana, T. Kolberg, G. Martinez, H. Prosper, C. Schiber, R. Yohay, J. Zhang

Florida Institute of Technology, Melbourne, USA

M.M. Baarmand, S. Butalla, T. Elkafrawy⁸⁴, M. Hohlmann, D. Noonan, M. Rahmani, M. Saunders, F. Yumiceva

University of Illinois at Chicago (UIC), Chicago, USA

M.R. Adams, L. Apanasevich, H. Becerril Gonzalez, R. Cavanaugh, X. Chen, S. Dittmer, O. Evdokimov, C.E. Gerber, D.A. Hangal, D.J. Hofman, C. Mills, G. Oh, T. Roy, M.B. Tonjes, N. Varelas, J. Viinikainen, X. Wang, Z. Wu

The University of Iowa, Iowa City, USA

M. Alhousseini, K. Dilsiz⁸⁵, S. Durgut, R.P. Gandrajula, M. Haytmyradov, V. Khristenko, O.K. Köseyan, J.-P. Merlo, A. Mestvirishvili⁸⁶, A. Moeller, J. Nachtman, H. Ogul⁸⁷, Y. Onel, F. Ozok⁸⁸, A. Penzo, C. Snyder, E. Tiras, J. Wetzel, K. Yi⁸⁹

Johns Hopkins University, Baltimore, USA

O. Amram, B. Blumenfeld, L. Corcodilos, M. Eminizer, A.V. Gritsan, S. Kyriacou, P. Maksimovic, C. Mantilla, J. Roskes, M. Swartz, T.Á. Vámi

The University of Kansas, Lawrence, USA

C. Baldenegro Barrera, P. Baringer, A. Bean, A. Bylinkin, T. Isidori, S. Khalil, J. King, G. Krintiras, A. Kropivnitskaya, C. Lindsey, N. Minafra, M. Murray, C. Rogan, C. Royon, S. Sanders, E. Schmitz, J.D. Tapia Takaki, Q. Wang, J. Williams, G. Wilson

Kansas State University, Manhattan, USA

S. Duric, A. Ivanov, K. Kaadze, D. Kim, Y. Maravin, T. Mitchell, A. Modak, A. Mohammadi

Lawrence Livermore National Laboratory, Livermore, USA

F. Rebassoo, D. Wright

University of Maryland, College Park, USA

E. Adams, A. Baden, O. Baron, A. Belloni, S.C. Eno, Y. Feng, N.J. Hadley, S. Jabeen, G.Y. Jeng, R.G. Kellogg, T. Koeth, A.C. Mignerey, S. Nabili, M. Seidel, A. Skuja, S.C. Tonwar, L. Wang, K. Wong

Massachusetts Institute of Technology, Cambridge, USA

D. Abercrombie, B. Allen, R. Bi, S. Brandt, W. Busza, I.A. Cali, Y. Chen, M. D'Alfonso, G. Gomez Ceballos, M. Goncharov, P. Harris, D. Hsu, M. Hu, M. Klute, D. Kovalskyi, J. Krupa, Y.-J. Lee, P.D. Luckey, B. Maier, A.C. Marini, C. McGinn, C. Mironov, S. Narayanan, X. Niu, C. Paus, D. Rankin, C. Roland, G. Roland, Z. Shi, G.S.F. Stephans, K. Sumorok, K. Tatar, D. Velicanu, J. Wang, T.W. Wang, Z. Wang, B. Wyslouch

University of Minnesota, Minneapolis, USA

R.M. Chatterjee, A. Evans, S. Guts[†], P. Hansen, J. Hiltbrand, Sh. Jain, M. Krohn, Y. Kubota, Z. Lesko, J. Mans, M. Revering, R. Rusack, R. Saradhy, N. Schroeder, N. Strobbe, M.A. Wadud

University of Mississippi, Oxford, USA

J.G. Acosta, S. Oliveros

University of Nebraska-Lincoln, Lincoln, USA

K. Bloom, S. Chauhan, D.R. Claes, C. Fangmeier, L. Finco, F. Golf, J.R. González Fernández, I. Kravchenko, J.E. Siado, G.R. Snow[†], B. Stieger, W. Tabb, F. Yan

State University of New York at Buffalo, Buffalo, USA

G. Agarwal, H. Bandyopadhyay, C. Harrington, L. Hay, I. Iashvili, A. Kharchilava, C. McLean, D. Nguyen, J. Pekkanen, S. Rappoccio, B. Roozbahani

Northeastern University, Boston, USA

G. Alverson, E. Barberis, C. Freer, Y. Haddad, A. Hortiangtham, J. Li, G. Madigan, B. Marzocchi, D.M. Morse, V. Nguyen, T. Orimoto, A. Parker, L. Skinnari, A. Tishelman-Charny, T. Wamorkar, B. Wang, A. Wisecarver, D. Wood

Northwestern University, Evanston, USA

S. Bhattacharya, J. Bueghly, Z. Chen, A. Gilbert, T. Gunter, K.A. Hahn, N. Odell, M.H. Schmitt, K. Sung, M. Velasco

University of Notre Dame, Notre Dame, USA

R. Bucci, N. Dev, R. Goldouzian, M. Hildreth, K. Hurtado Anampa, C. Jessop, D.J. Karmgard, K. Lannon, W. Li, N. Loukas, N. Marinelli, I. Mcalister, F. Meng, K. Mohrman, Y. Musienko⁴⁶, R. Ruchti, P. Siddireddy, S. Taroni, M. Wayne, A. Wightman, M. Wolf, L. Zygala

The Ohio State University, Columbus, USA

J. Alimena, B. Bylsma, B. Cardwell, L.S. Durkin, B. Francis, C. Hill, A. Lefeld, B.L. Winer, B.R. Yates

Princeton University, Princeton, USA

P. Das, G. Dezoort, P. Elmer, B. Greenberg, N. Haubrich, S. Higginbotham, A. Kalogeropoulos, G. Kopp, S. Kwan, D. Lange, M.T. Lucchini, J. Luo, D. Marlow, K. Mei, I. Ojalvo, J. Olsen, C. Palmer, P. Piroué, D. Stickland, C. Tully

University of Puerto Rico, Mayaguez, USA

S. Malik, S. Norberg

Purdue University, West Lafayette, USA

V.E. Barnes, R. Chawla, S. Das, L. Gutay, M. Jones, A.W. Jung, B. Mahakud, G. Negro, N. Neumeister, C.C. Peng, S. Piperov, H. Qiu, J.F. Schulte, M. Stojanovic¹⁶, N. Trevisani, F. Wang, R. Xiao, W. Xie

Purdue University Northwest, Hammond, USA

T. Cheng, J. Dolen, N. Parashar

Rice University, Houston, USA

A. Baty, S. Dildick, K.M. Ecklund, S. Freed, F.J.M. Geurts, M. Kilpatrick, A. Kumar, W. Li, B.P. Padley, R. Redjimi, J. Roberts[†], J. Rorie, W. Shi, A.G. Stahl Leiton

University of Rochester, Rochester, USA

A. Bodek, P. de Barbaro, R. Demina, J.L. Dulemba, C. Fallon, T. Ferbel, M. Galanti, A. Garcia-Bellido, O. Hindrichs, A. Khukhunaishvili, E. Ranken, R. Taus

Rutgers, The State University of New Jersey, Piscataway, USA

B. Chiarito, J.P. Chou, A. Gandrakota, Y. Gershtein, E. Halkiadakis, A. Hart, M. Heindl, E. Hughes, S. Kaplan, O. Karacheban²⁴, I. Laflotte, A. Lath, R. Montalvo, K. Nash, M. Osherson, S. Salur, S. Schnetzer, S. Somalwar, R. Stone, S.A. Thayil, S. Thomas, H. Wang

University of Tennessee, Knoxville, USA

H. Acharya, A.G. Delannoy, S. Spanier

Texas A&M University, College Station, USA

O. Bouhali⁹⁰, M. Dalchenko, A. Delgado, R. Eusebi, J. Gilmore, T. Huang, T. Kamon⁹¹, H. Kim, S. Luo, S. Malhotra, R. Mueller, D. Overton, L. Perniè, D. Rathjens, A. Safonov, J. Sturdy

Texas Tech University, Lubbock, USA

N. Akchurin, J. Damgov, V. Hegde, S. Kunori, K. Lamichhane, S.W. Lee, T. Mengke, S. Muthumuni, T. Peltola, S. Undleeb, I. Volobouev, Z. Wang, A. Whitbeck

Vanderbilt University, Nashville, USA

E. Appelt, S. Greene, A. Gurrola, R. Janjam, W. Johns, C. Maguire, A. Melo, H. Ni, K. Padeken, F. Romeo, P. Sheldon, S. Tuo, J. Velkovska, M. Verweij

University of Virginia, Charlottesville, USA

M.W. Arenton, B. Cox, G. Cummings, J. Hakala, R. Hirosky, M. Joyce, A. Ledovskoy, A. Li, C. Neu, B. Tannenwald, Y. Wang, E. Wolfe, F. Xia

Wayne State University, Detroit, USA

R. Harr, P.E. Karchin, N. Poudyal, P. Thapa

University of Wisconsin - Madison, Madison, WI, USA

K. Black, T. Bose, J. Buchanan, C. Caillol, S. Dasu, I. De Bruyn, P. Everaerts, C. Galloni, H. He, M. Herndon, A. Hervé, U. Hussain, A. Lanaro, A. Loeliger, R. Loveless, J. Madhusudanan Sreekala, A. Mallampalli, D. Pinna, T. Ruggles, A. Savin, V. Shang, V. Sharma, W.H. Smith, D. Teague, S. Trembath-reichert, W. Vetens

†: Deceased

- 1: Also at Vienna University of Technology, Vienna, Austria
- 2: Also at Department of Basic and Applied Sciences, Faculty of Engineering, Arab Academy for Science, Technology and Maritime Transport, Alexandria, Egypt
- 3: Also at Université Libre de Bruxelles, Bruxelles, Belgium
- 4: Also at IRFU, CEA, Université Paris-Saclay, Gif-sur-Yvette, France
- 5: Also at Universidade Estadual de Campinas, Campinas, Brazil
- 6: Also at Federal University of Rio Grande do Sul, Porto Alegre, Brazil
- 7: Also at UFMS, Nova Andradina, Brazil
- 8: Also at Universidade Federal de Pelotas, Pelotas, Brazil
- 9: Also at University of Chinese Academy of Sciences, Beijing, China
- 10: Also at Institute for Theoretical and Experimental Physics named by A.I. Alikhanov of NRC 'Kurchatov Institute', Moscow, Russia
- 11: Also at Joint Institute for Nuclear Research, Dubna, Russia
- 12: Also at Helwan University, Cairo, Egypt
- 13: Now at Zewail City of Science and Technology, Zewail, Egypt
- 14: Now at British University in Egypt, Cairo, Egypt
- 15: Now at Cairo University, Cairo, Egypt
- 16: Also at Purdue University, West Lafayette, USA
- 17: Also at Université de Haute Alsace, Mulhouse, France
- 18: Also at Ilia State University, Tbilisi, Georgia
- 19: Also at Erzincan Binali Yildirim University, Erzincan, Turkey
- 20: Also at CERN, European Organization for Nuclear Research, Geneva, Switzerland
- 21: Also at RWTH Aachen University, III. Physikalisches Institut A, Aachen, Germany
- 22: Also at University of Hamburg, Hamburg, Germany
- 23: Also at Department of Physics, Isfahan University of Technology, Isfahan, Iran, Isfahan, Iran
- 24: Also at Brandenburg University of Technology, Cottbus, Germany
- 25: Also at Skobeltsyn Institute of Nuclear Physics, Lomonosov Moscow State University, Moscow, Russia
- 26: Also at Institute of Physics, University of Debrecen, Debrecen, Hungary, Debrecen, Hungary
- 27: Also at Physics Department, Faculty of Science, Assiut University, Assiut, Egypt
- 28: Also at MTA-ELTE Lendület CMS Particle and Nuclear Physics Group, Eötvös Loránd University, Budapest, Hungary, Budapest, Hungary
- 29: Also at Institute of Nuclear Research ATOMKI, Debrecen, Hungary
- 30: Also at IIT Bhubaneswar, Bhubaneswar, India, Bhubaneswar, India
- 31: Also at Institute of Physics, Bhubaneswar, India
- 32: Also at G.H.G. Khalsa College, Punjab, India
- 33: Also at Shoolini University, Solan, India
- 34: Also at University of Hyderabad, Hyderabad, India
- 35: Also at University of Visva-Bharati, Santiniketan, India
- 36: Also at Indian Institute of Technology (IIT), Mumbai, India
- 37: Also at Deutsches Elektronen-Synchrotron, Hamburg, Germany

-
- 38: Also at Department of Physics, University of Science and Technology of Mazandaran, Behshahr, Iran
- 39: Now at INFN Sezione di Bari ^a, Università di Bari ^b, Politecnico di Bari ^c, Bari, Italy
- 40: Also at Italian National Agency for New Technologies, Energy and Sustainable Economic Development, Bologna, Italy
- 41: Also at Centro Siciliano di Fisica Nucleare e di Struttura Della Materia, Catania, Italy
- 42: Also at INFN Sezione di Napoli ^a, Università di Napoli 'Federico II' ^b, Napoli, Italy, Università della Basilicata ^c, Potenza, Italy, Università G. Marconi ^d, Roma, Italy, Napoli, Italy
- 43: Also at Riga Technical University, Riga, Latvia, Riga, Latvia
- 44: Also at Consejo Nacional de Ciencia y Tecnología, Mexico City, Mexico
- 45: Also at Warsaw University of Technology, Institute of Electronic Systems, Warsaw, Poland
- 46: Also at Institute for Nuclear Research, Moscow, Russia
- 47: Now at National Research Nuclear University 'Moscow Engineering Physics Institute' (MEPhI), Moscow, Russia
- 48: Also at St. Petersburg State Polytechnical University, St. Petersburg, Russia
- 49: Also at University of Florida, Gainesville, USA
- 50: Also at Imperial College, London, United Kingdom
- 51: Also at P.N. Lebedev Physical Institute, Moscow, Russia
- 52: Also at Moscow Institute of Physics and Technology, Moscow, Russia, Moscow, Russia
- 53: Also at California Institute of Technology, Pasadena, USA
- 54: Also at Budker Institute of Nuclear Physics, Novosibirsk, Russia
- 55: Also at Faculty of Physics, University of Belgrade, Belgrade, Serbia
- 56: Also at Trincomalee Campus, Eastern University, Sri Lanka, Nilaveli, Sri Lanka
- 57: Also at INFN Sezione di Pavia ^a, Università di Pavia ^b, Pavia, Italy, Pavia, Italy
- 58: Also at National and Kapodistrian University of Athens, Athens, Greece
- 59: Also at Universität Zürich, Zurich, Switzerland
- 60: Also at Stefan Meyer Institute for Subatomic Physics, Vienna, Austria, Vienna, Austria
- 61: Also at Laboratoire d'Annecy-le-Vieux de Physique des Particules, IN2P3-CNRS, Annecy-le-Vieux, France
- 62: Also at Şırnak University, Şırnak, Turkey
- 63: Also at Department of Physics, Tsinghua University, Beijing, China, Beijing, China
- 64: Also at Near East University, Research Center of Experimental Health Science, Nicosia, Turkey
- 65: Also at Beykent University, Istanbul, Turkey, Istanbul, Turkey
- 66: Also at Istanbul Aydın University, Application and Research Center for Advanced Studies (App. & Res. Cent. for Advanced Studies), Istanbul, Turkey
- 67: Also at Mersin University, Mersin, Turkey
- 68: Also at Piri Reis University, Istanbul, Turkey
- 69: Also at Adiyaman University, Adiyaman, Turkey
- 70: Also at Ozyegin University, Istanbul, Turkey
- 71: Also at Izmir Institute of Technology, Izmir, Turkey
- 72: Also at Necmettin Erbakan University, Konya, Turkey
- 73: Also at Bozok Universitetesi Rektörlüğü, Yozgat, Turkey
- 74: Also at Marmara University, Istanbul, Turkey
- 75: Also at Milli Savunma University, Istanbul, Turkey
- 76: Also at Kafkas University, Kars, Turkey
- 77: Also at Istanbul Bilgi University, Istanbul, Turkey
- 78: Also at Hacettepe University, Ankara, Turkey
- 79: Also at School of Physics and Astronomy, University of Southampton, Southampton,

United Kingdom

- 80: Also at IPPP Durham University, Durham, United Kingdom
- 81: Also at Monash University, Faculty of Science, Clayton, Australia
- 82: Also at Bethel University, St. Paul, Minneapolis, USA, St. Paul, USA
- 83: Also at Karamanoğlu Mehmetbey University, Karaman, Turkey
- 84: Also at Ain Shams University, Cairo, Egypt
- 85: Also at Bingol University, Bingol, Turkey
- 86: Also at Georgian Technical University, Tbilisi, Georgia
- 87: Also at Sinop University, Sinop, Turkey
- 88: Also at Mimar Sinan University, Istanbul, Istanbul, Turkey
- 89: Also at Nanjing Normal University Department of Physics, Nanjing, China
- 90: Also at Texas A&M University at Qatar, Doha, Qatar
- 91: Also at Kyungpook National University, Daegu, Korea, Daegu, Korea